1-2019

Tooth development and replacement in the Atlantic Cutlassfish, Trichiurus lepturus, with comparisons to other Scombroidei

Katherine E. Bemis
Virginia Institute of Marine Science

Samantha M. Burke

Carl A. St John

Eric J. Hilton
Virginia Institute of Marine Science

William E. Bemis

Recommended Citation

Bemis, Katherine E.; Burke, Samantha M.; St John, Carl A.; Hilton, Eric J.; and Bemis, William E., Tooth development and replacement in the Atlantic Cutlassfish, Trichiurus lepturus, with comparisons to other Scombroidei (2019). *Journal of Morphology*, 280(1), 78-94.
10.1002/jmor.20919

Received: 6 April 2018 | Revised: 17 October 2018 | Accepted: 27 October 2018

DOI: 10.1002/jmor.20919

WILEY morphology

RESEARCH ARTICLE

Tooth development and replacement in the Atlantic Cutlassfish, *Trichiurus lepturus*, with comparisons to other Scombroidei

Katherine E. Bemis[1] | Samantha M. Burke[2] | Carl A. St. John[2] | Eric J. Hilton[1] | William E. Bemis[3]

[1]Department of Fisheries Science, Virginia Institute of Marine Science, College of William & Mary, Gloucester Point, Virginia

[2]Department of Ecology and Evolutionary Biology, Cornell University, Ithaca, New York

[3]Department of Ecology and Evolutionary Biology and Cornell University Museum of Vertebrates, Cornell University, Ithaca, New York

Correspondence
Katherine E. Bemis, Department of Fisheries Science, Virginia Institute of Marine Science, College of William & Mary, P.O. Box 1346, Gloucester Point, VA 23062.
Email: kebemis@vims.edu

Funding information
Cornell University Jane E. Brody Undergraduate Research Grant; Cornell University Morley Student Research Grant; National Science Foundation Graduate Research Fellowship; Tontogany Creek Fund; VIMS Foundation Nancy S. and Henry George Fellowship

Abstract

Atlantic Cutlassfish, *Trichiurus lepturus*, have large, barbed, premaxillary and dentary fangs, and sharp dagger-shaped teeth in their oral jaws. Functional teeth firmly ankylose to the dentigerous bones. We used dry skeletons, histology, SEM, and micro-CT scanning to study 92 specimens of *T. lepturus* from the western North Atlantic to describe its dentition and tooth replacement. We identified three modes of intraosseous tooth replacement in *T. lepturus* depending on the location of the tooth in the jaw. Mode 1 relates to replacement of premaxillary fangs, in which new tooth germs enter the lingual surface of the premaxilla, develop horizontally, and rotate into position. We suggest that growth of large fangs in the premaxilla is accommodated by this horizontal development. Mode 2 occurs for dentary fangs: new tooth germs enter the labial surface of the dentary, develop vertically, and erupt into position. Mode 3 describes replacement of lateral teeth, in which new tooth germs enter a trench along the crest of the dentigerous bone, develop vertically, and erupt into position. Such distinct modes of tooth replacement in a teleostean species are unknown. We compared modes of replacement in *T. lepturus* to 20 species of scombroids to explore the phylogenetic distribution of these three replacement modes. Alternate tooth replacement (in which new teeth erupt between two functional teeth), ankylosis, and intraosseous tooth development are plesiomorphic to Bluefish + other Scombroidei. Our study highlights the complexity and variability of intraosseous tooth replacement. Within tooth replacement systems, key variables include sites of formation of tooth germs, points of entry of tooth germs into dentigerous bones, coupling of tooth germ migration and bone erosion, whether teeth develop horizontally or immediately beneath the tooth to be replaced, and how tooth eruption and ankylosis occur. Developmentally different tooth replacement processes can yield remarkably similar dentitions.

KEYWORDS

alternate tooth replacement, bone remodeling, intraosseous tooth replacement, micro-CT scanning, Trichiuridae

1 | INTRODUCTION

Teleostean fishes continuously replace teeth throughout life (Bemis, Giuliano, & McGuire, 2005; Berkovitz & Shellis, 2017; Huysseune & Witten, 2006). Extraosseous and intraosseous tooth replacement are two main patterns used to characterize tooth replacement (Trapani, 2001), although these may be extremes of a continuum (Conway, Bertrand, Browning, Lancon, & Clubb, 2015). In this article, we focus on intraosseous tooth replacement in the oral jaws, which has evolved in at least three clades of teleosts (Trapani, 2001). In some documented instances of intraosseous replacement, such as the Bluefish, *Pomatomus saltatrix*, new tooth germs form directly in association with the oral epithelium (Bemis et al., 2005). The new tooth germ and associated cells then erode a replacement pore through which they move

into the medullary cavity of the dentigerous bone while still connected to the oral epithelium by the dental lamina (Figure 1). The new tooth continues to develop and eventually erupts and replaces the functional tooth through bone remodeling. In fishes with a single row of teeth, tooth germs can enter the dentigerous bone from either the lingual or labial side of the jaw (Figure 1). If there are multiple rows of teeth, then tooth germs can enter from both sides of the dentigerous bone (e.g., Atlantic Wolffish, *Anarhichas lupus*, Bemis & Bemis, 2015). This variation may be phylogenetically informative, but the position of new tooth germs and replacement pores has not been widely surveyed or considered in a phylogenetic context (Bemis et al., 2005; Thiery et al., 2017).

Cutlassfishes are pelagic ambush predators that primarily feed on cephalopods and bony fishes as adults (Martins, Haimovici, & Palacios, 2005). The Atlantic Cutlassfish, *Trichiurus lepturus*, occurs in warm coastal shelf waters around the world (Nakamura & Parin, 1993). The heterodont dentition of *T. lepturus* consists of large, barbed, premaxillary, and dentary fangs positioned anteriorly in the jaw, and laterally compressed dagger-shaped teeth posteriorly, which in larger individuals

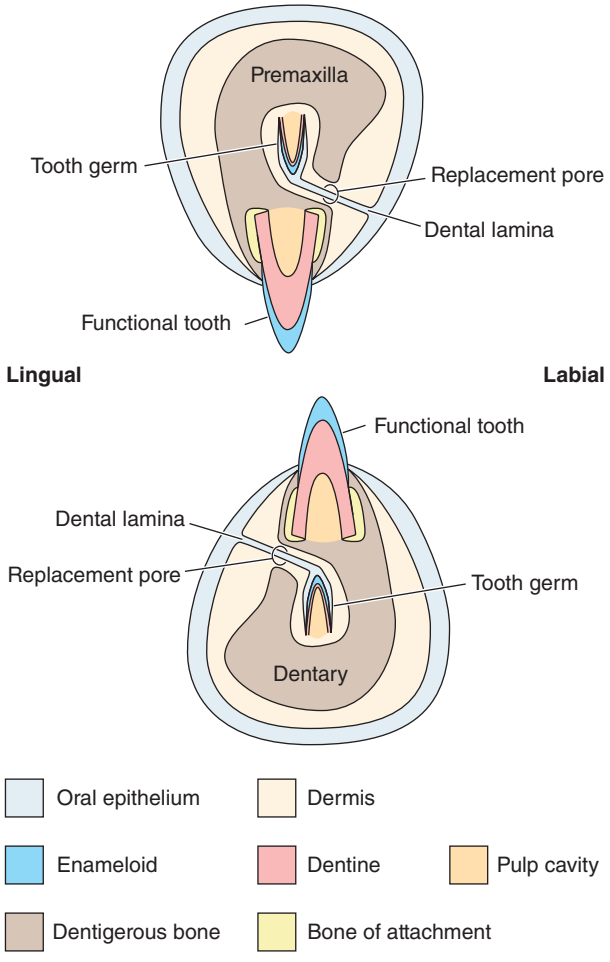

FIGURE 1 Overview of intraosseous replacement of oral teeth based on Bluefish, *Pomatomus saltatrix*. During intraosseous tooth replacement, tooth germs migrate into dentigerous bones through a replacement pore. Location of replacement pores varies within teleosts: they can occur, for example, on the lingual or labial surfaces of the bones. In Bluefish, new tooth germs form on the labial side of the premaxilla and the lingual side of the dentary

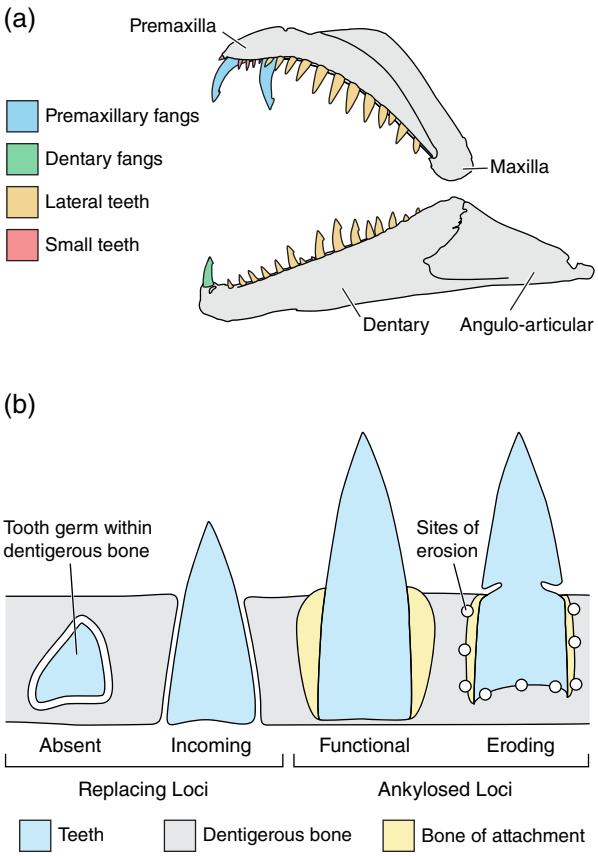

FIGURE 2 Morphological data and terminology used in this study. (a) Diagram showing four types of teeth in the oral jaws of *Trichiurus lepturus*. (b) Diagram of developing teeth based on Morgan and King (1983), simplified and relabeled to match tooth classification system of Bemis et al. (2005; A, I, F, E) used here. Replacing Loci are those scored A or I. Ankylosed Loci are those scored F or E

can also bear barbs (Figure 2a). Morgan (1977, pp. 73) described the dentition and tooth replacement patterns in *T. lepturus* and specified that "tooth development occurs in the dentigerous bones" (intraosseous replacement) and that intraosseous development is an adaptation that prevents struggling prey from dislodging developing teeth. Morgan (1977) described the unusual intraosseous replacement that occurs for the premaxillary fangs, which develop horizontally and rotate into place. Here, we provide new anatomical and developmental data and phylogenetic context for intraosseous tooth replacement modes of *T. lepturus* based on a large series of individuals to document stages and variation. We also compare modes of tooth replacement in *T. lepturus* to those of related taxa to understand the phylogenetic distribution of these replacement modes.

2 | MATERIALS AND METHODS

2.1 | Terminology

We use bone of attachment to refer to the tissue connecting the dentine of a tooth to the dentigerous bone (e.g., dentary; sensu Sire and Huysseune, 2003, pp. 236; also see Hall, 2015: fig. 1.1—note that the basal bone of Hall, 2015, is referred to as dentigerous bone here).

Ankylosis is achieved when the ligaments connecting the bone of attachment to the dentigerous bone are mineralized; such ankylosis corresponds to tooth attachment Type 1 of Fink (1981). We follow Tucker (1956) who used the term "fang" to refer to large teeth in the front of the premaxillae and dentaries in trichiurids. The term "fang" also has been used to describe large teeth in different groups of teleost fishes (i.e., "fangs" in different taxa do not necessarily look the same, see descriptions in Nakamura & Parin, 1993 for Gempylidae and Trichiuridae; Melo, 2009 for Chiasmodontidae; and Grande, 2010 for Lepisosteidae), however, all are united by their relatively large size in comparison to other teeth, and their anterior positions in the jaw. Morgan (1977) used the term "barb" to describe the hook-shaped enameloid cap of some but not all teeth in the dentition of *Trichiurus lepturus*, and we follow his usage here. In barbed teeth, there is an enameloid keel only on the anterior cutting edge of the tooth. In contrast, unbarbed teeth have prominent enameloid keels on both the anterior and posterior cutting edges. We use the term "locus" to refer to a single position on a dentigerous bone where teeth will or have already erupted (Bemis et al., 2005). Typically, a locus in species with intraosseous tooth replacement is a position for multiple generations of teeth throughout an individual's lifetime; in *T. lepturus*, more loci can be added posterior to the existing loci as a fish grows.

We follow phylogenetic interpretations of Orrell, Collette, and Johnson (2006: fig. 2), who concluded that billfishes are not part of Scombroidei, and that Bluefish, *Pomatomus saltatrix*, and Longfin Escolar, *Scombrolabrax heterolepis*, are at the base of a clade including Gempylidae, Trichiuridae, and Scombridae. Most recent molecular analyses (e.g., Betancur-R et al., 2017) recover a monophyletic group containing *Trichiurus lepturus* + *Gempylus serpens*, two taxa studied here, but Miya et al. (2013) report a different and nonmonophyletic arrangement; however, neither of these studies was designed to test monophyly of Gempylidae and Trichiuridae, and have low taxon sampling given the species diversity of each proposed family. Recently, Beckett et al. (2018) analyzed new morphological characters combined with mtDNA data from Miya et al. (2013) and reported that "Gempylidae" is not monophyletic, and that Trichiuridae is a clade within "Gempylidae." In their strict consensus tree of morphological data (Beckett et al., 2018: fig. 13B), *P. saltatrix* and *S. heterolepis* are placed in a polytomy with Scombridae (represented by *Gasterochisma melampus*) and "Gempylidae" including Trichiuridae. For our analyses, we interpret that *G. serpens* and *T. lepturus* are members of a monophyletic group within Scombroidei.

2.2 | Examined specimens of *Trichiurus lepturus*

We prepared 79 specimens of *Trichiurus lepturus* Linnaeus, 1758, ranging from 514 to 1,110 mm TL (total length), caught by bottom trawl surveys conducted by the Northeast Fisheries Science Center (Politis, Galbraith, Kostovick, & Brown, 2014). Specimens were fixed in 10% formalin (n = 7) or frozen at sea (n = 72). All specimens are deposited in the Nunnally Ichthyology Collection at the Virginia Institute of Marine Science (VIMS; see Appendix). We examined 13 larval specimens ranging from 5 to 37 mm TL from the Southeast Area Monitoring and Assessment Program (SEAMAP/SML); these were collected during monitoring programs in the Gulf of Mexico. We also studied two juvenile specimens, 220 and 240 mm TL (VIMS 35823), collected in Chesapeake Bay.

2.3 | Measurements and scoring

We dissected 72 specimens of *Trichiurus lepturus*, measured TL, recorded sex based on examination of gonads (M = male; F = female), and prepared dry skeletons (Bemis et al., 2004). For 15 specimens, we counted the number of loci, scored the replacement status of each locus, and the positions of replacement pores (sensu Bemis et al., 2005). As shown in Figure 2b, we used the replacement classification of Bemis et al. (2005), which is: Absent (A, locus empty or shows broken remnants of previous tooth generation and the new tooth is developing within the bone); Incoming (I, tooth crown visible above the dentigerous bone but tooth is not ankylosed); Functional (F, tooth fully ankylosed around its circumference); or Eroding (E, ankylosis eroding around its circumference or at the base of the tooth). Both Absent and Incoming loci can be characterized as Replacing Loci (Figure 2b); they are either wholly within the jaw or incompletely erupted, not ankylosed, and thus likely do not contribute to feeding. Functional and Eroding loci collectively make up Ankylosed Loci (Figure 2b), and the teeth in such loci can be used in feeding. We measured tooth height (above the jaw) and base length (along the jaw) for Functional and Eroding teeth. We scored the presence of barbs on all Functional and Eroding teeth; if an Incoming tooth was sufficiently erupted to see a barb, then we scored it. Absent and Incoming loci in which the barb could not be seen were not scored. This scoring system yielded a minimal estimate of the number of barbed lateral teeth in the dentary, particularly for specimens in which the loci of the barbed region were in an early stage of a replacement wave. A replacement wave consists of two or more alternate loci with teeth in similar stages of development or progressive stages in a series (e.g., Functional teeth in loci 1, 3, and 5 would be an example of three alternate loci within the same replacement wave). We graphically identified tooth replacement waves by connecting dashed lines between alternate loci in plots of locus condition.

2.4 | Micro-computed tomography

We scanned three specimens with micro-CT: (a) the head of a specimen fixed in formalin and then dehydrated in ethanol before air drying (VIMS 35783); (b) a dry skeletal preparation of a premaxilla (VIMS 35776); and (c) a single premaxillary fang (VIMS 35784). We used a GE 120 micro-CT scanner in the Biotechnology Resource Center Multiscale Imaging Facility at Cornell University to prepare data sets for VIMS 35783. Reconstructions prepared from these data sets have a resolution of 50–100 μm voxels. We used the facility's Xradia Versa XRM-500 nano-CT scanner to prepare data sets for VIMS 35776 and VIMS 35784, with resolutions of 5–20 μm voxels. We made 2D orthogonal MPR (multiplanar reformatting) and 3D volume reconstructions using OsiriX™ (version 5.8.5, 64-bit edition) DICOM imaging software (Rosset, Spadola, & Ratib, 2004) on Apple Macintosh computers running OSX 10.8.5. To view internal anatomy of teeth and bones, we digitally dissected reconstructions within OsiriX™.

2.5 | Histology and Scanning Electron Microscopy

We decalcified portions of two formalin-fixed specimens using Formic Acid A (Humason, 1972; 20% formic acid), washed and dehydrated them for paraffin embedding, cut sections at 6 μm, and stained them with H&E (hematoxylin and eosin; Cornell Veterinary College Diagnostic Laboratory). For SEM study, we washed portions of dry skeletal specimen VIMS 35776 in several changes of household ammonia and water before dehydration in acetone and air drying. We mounted targeted parts of the specimen on stubs, sputter coated them with gold palladium, and imaged them with a JEOL NeoScope JCM-5000 SEM at the Paleontological Research Institution (PRI, Ithaca, NY).

2.6 | Hardness testing

We performed hardness testing at the Cornell Center for Materials Research using a diamond indenter (Nanovea Series Digital Microhardness Tester HWMMT-X3). Teeth from VIMS 35784 were embedded in epoxy and the surface was ground flat using a graded series of carborundum grits. We measured dimensions of the indentations to calculate Vickers hardness (Bemis, 1984).

2.7 | Comparative materials

We studied dry skeletal materials and preserved specimens of representative scombroids from 20 species in 18 genera (see Appendix). The intent of our comparisons is not to provide detailed studies of all scombroid dentitions, but to focus on modes of tooth replacement.

2.8 | Photography

We photographed sections using an Olympus SZX12 microscope equipped with an Olympus DP70 digital camera. We used a Canon 5D Mark II digital camera to record color macrophotographs. Using Adobe Photoshop CS6, we adjusted images for color balance and contrast, and prepared plates and line drawings in Adobe Illustrator CS6.

3 | RESULTS

We found teeth in specimens >6 mm TL (e.g., SML 450916-000, 5 mm TL, lacks teeth). The silver-pigmented skin covering the tooth-bearing bones of the jaws is extremely thin (Figure 3a). As a result, the major skeletal elements (Figure 3b) are visible even with the skin intact. The long dentaries extend anteriorly beyond the premaxillae (Figure 3), so that the mandibular symphysis is the most anterior point on the head. Elongate premaxillary and dentary fangs are approximately perpendicular to their dentigerous bones when they are fully ankylosed. When the jaw is closed, the premaxillary fangs fit into recesses in the soft tissue between the rami of the lower jaw. The anteriormost premaxillary fangs fit anterior to a pair of distinct medial bony thickenings near the symphysis of the left and right dentary bones. The second or third functional premaxillary fangs insert posterior to these thickenings. Dentary fangs do not contact the premaxillary fangs because the dentary is longer. There is a small tooth on each premaxilla in front of the anteriormost fang, and a series of small teeth between and lateral to the premaxillary fangs (Figure 3b). Posteriorly along the premaxilla is the series of teeth that we term lateral teeth. A corresponding series of lateral teeth is posterior to the dentary fangs, but the dentary lacks small teeth comparable to those in the anterior portion of the premaxilla.

3.1 | Premaxillary fangs and replacement

Each premaxilla has three loci for large barbed fangs (Figure 4). Vascular dentine makes up most of the tooth, but a dense outer enameloid layer forms a sharp blade along the anterior edges of the fangs, which we term a keel (Figure 5). The keel is a smooth cutting edge, without serrations. In the premaxillary fangs, the enameloid keel continues into the barb and extends along the barb's posterior edge (Figure 5a), but proximal to the barb, the posterior edge of the fang is rounded, without a keel or any evidence of dense mineralization. Diamond-indenter hardness testing showed that average Vickers hardness (HV) of the barb is 213 HV ($SD \pm 44$) in comparison to the shaft, which has a hardness of 53 HV ($SD \pm 3$; Figure 6).

In most specimens examined, no more than two of the three premaxillary loci had ankylosed fully functional fangs (Figure 4), with the other fang locus or loci undergoing replacement (Figure 7). We observed some cases in which three functional fangs were present (e.g., Figure 7ɳ, o). We interpret that the premaxillary fangs have an alternate replacement pattern. Replacement pores are located on the lingual side of the premaxilla. For example, two replacement pores (1RP and 3RP) are visible in Figure 4a; tooth germs have already migrated into the bone through these pores.

The premaxillary fangs exhibit intraosseous tooth replacement in which they develop horizontally along the axis of the premaxilla. The tip of the incoming fang (2I; Figure 4a) faces posteriorly, and, as it develops, it grows out of the replacement pore through which its tooth germ originally migrated into the premaxilla. The tooth reaches full size before rotating into position and ankylosing. In Figure 4a, tooth 2I has nearly completed its development. As a premaxillary fang reaches full size, a channel erodes in the bone allowing the fang to rotate ventrally to a nearly perpendicular position before ankylosing to the premaxilla (Figure 4b). Teeth that have recently rotated into place and have yet to ankylose to the dentigerous bone can be depressed by light pressure from a probe. The large channels created by new teeth rotating into place weaken the attachment of adjacent fangs from earlier generations, and their attachments begin to give way. In the two juvenile specimens examined (220 and 240 mm TL; VIMS 35823), horizontal tooth replacement of premaxillary fangs is evident.

3.2 | Dentary fangs and replacement

Each dentary bears a single ankylosed barbed fang. A diastema separates the fang from the single row of lateral teeth along the dentary crest, and premaxillary fangs overlap the diastema (Figure 3). Dentary fangs have a second mode of replacement (Figures 7–9). All 92 specimens examined had two loci for dentary fangs (Figure 7). One locus always had an ankylosed fang and the other locus was in a replacement stage, yielding an alternate pattern of replacement. New tooth

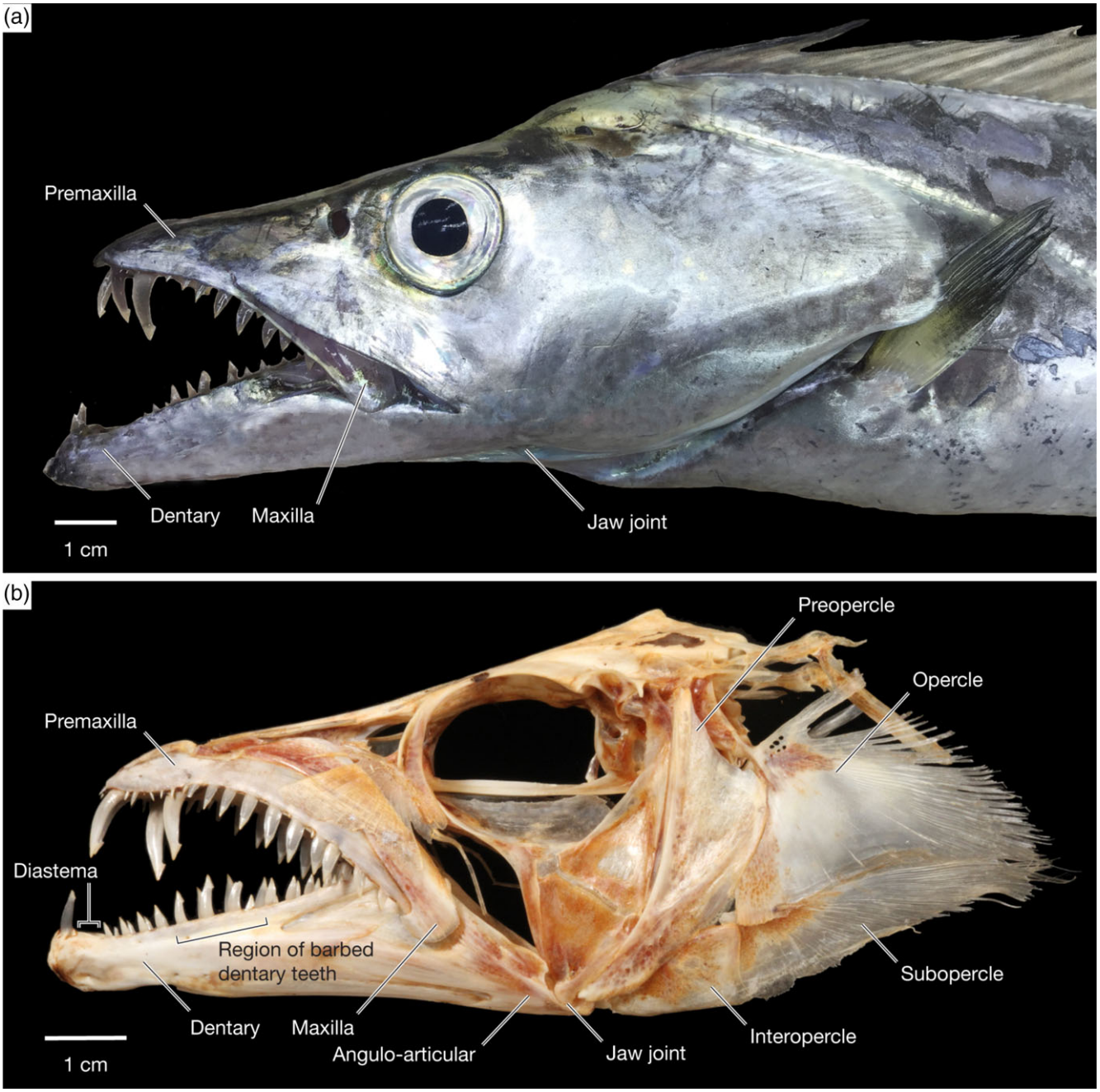

FIGURE 3 *Trichiurus lepturus*, head and dentition of adult specimens. (a) Lateral view of freshly caught specimen to show external anatomy of head with intact soft tissues. VIMS 35902, 1,045 mm SL. (b) Lateral view of cranial skeleton to show general arrangement of dentigerous bones and teeth (right side of specimen is shown; image has been reversed so that anterior faces left). VIMS 35789, 964 mm TL, F

germs erode a well-developed replacement pore to enter the dentary on its labial side (Figure 8). Once the tooth germ enters through the replacement pore, the new fang develops within the dentary and erupts vertically, directly into the locus (Figures 8 and 9). Dentary fangs never rotate unlike the developing premaxillary fangs. The replacement pore of a dentary fang remains open throughout the replacement process, and its diameter increases as the incoming tooth begins to erupt through it into position, until the tooth reaches its full height and ankylosis begins. The smooth surfaces of the replacement pore and eroding surface for the incoming fang are the result of osteoclast activity during erosion of the existing bone to accommodate the migrating tooth germ (Figures 8 and 9).

In the specimen shown in Figure 9, the dentary fang is ankylosed to the surrounding bone of the dentary, but its base is already being eroded. The skin of the lower jaw is exceptionally thin, and there are no pads flanking the labial surface of the ankylosed fang. Lingually, there is a thin pad-like gum with adipose tissue deep to it.

3.3 | Lateral teeth and replacement

The lateral teeth of the premaxilla and dentary are deeply socketed and ankylosed in a trench along the crest of the dentigerous bone (Figure 4b). The lateral teeth are laterally compressed with cutting edges on their anterior and posterior surfaces, but only some teeth in the dentary are barbed.

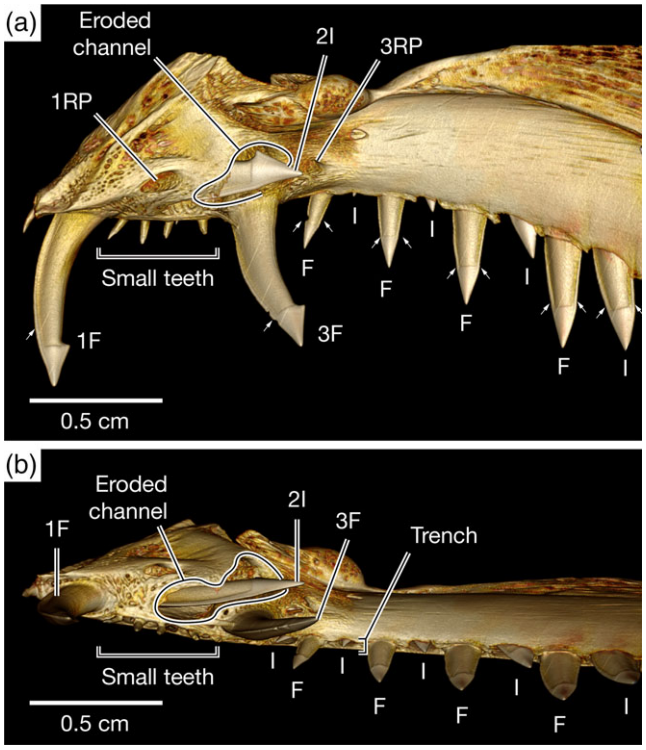

FIGURE 4 *Trichiurus lepturus*, micro-CT reconstruction of dentition and tooth replacement in right premaxilla. (a) Lingual view, anterior to left. Two functional ankylosed fangs are present (1F, 3F), each with a replacement pore (1RP, 3RP) posterior to the corresponding fang. The incoming fang at the second locus (2I) is horizontal and aligned with the ramus of the premaxilla. A series of small teeth extend laterally between the three fang loci; a single small tooth is located at the anterior tip of the premaxilla. Incoming (I) lateral teeth alternate with Functional (F) lateral teeth; note that the incoming lateral teeth are just beginning to erupt in the anterior part of the series and have almost completed eruption posteriorly. This difference reflects a replacement wave. Arrows indicate enameloid keel(s) of teeth; in barbed teeth, there is a keel only on the anterior cutting edge of the tooth. Unbarbed teeth have enameloid keels on both the anterior and posterior cutting edges. (b) Palatal (ventral) view of the same specimen shown in (a). The incoming fang (2I) is eroding a channel in the premaxilla, through which the fang will rotate into position. The incoming lateral teeth are erupting via the trench along the crest of the premaxilla. VIMS 35776, 540 mm TL, M

Figure 10 plots the condition (A, I, F, E) for a series of 15 specimens ranging from 514 to 1,103 mm TL. The total number of premaxillary loci for lateral teeth ranged from 15 (Figure 10b) to 23 (Figure 10l). The number of dentary loci for lateral teeth ranged from 16 (Figure 10c) to 29 (Figure 10n). Within each specimen, the number of loci for lateral teeth in the premaxilla correlated with the number of loci for lateral teeth in the dentary (r^2 = .86). For example, specimens that have few premaxillary loci also have few dentary loci (Figure 10c). The number of premaxillary and dentary loci correlates with TL (r^2 = .76 and .79, respectively). No statistically significant relationship was found between number of loci of lateral teeth and sex of the individual, that is, male and female specimens of similar lengths have similar numbers of loci. For example, two of the largest specimens examined are male and female (Figure 10k,l, respectively), and they have similar numbers of loci for lateral teeth in the premaxilla and dentary.

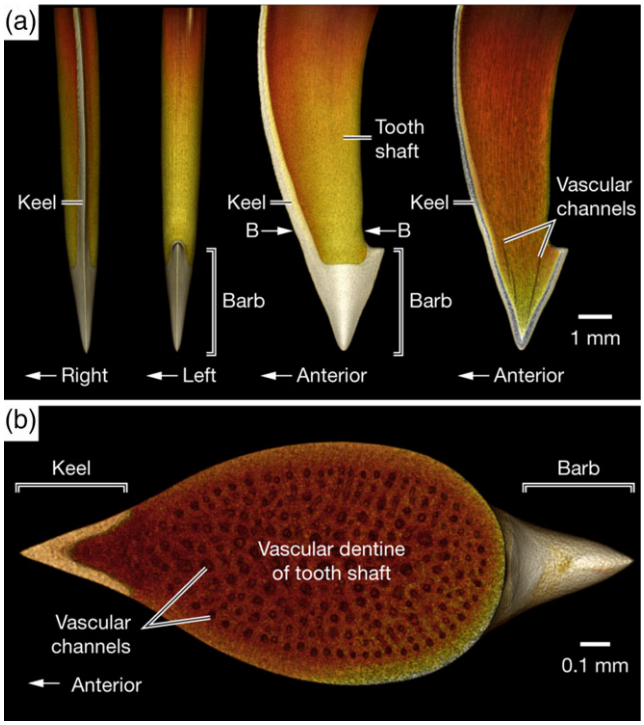

FIGURE 5 *Trichiurus lepturus*, micro-CT reconstruction and virtual dissection of a fang from the left premaxilla. Lighter colors indicate greater tissue density. (a) Anterior, posterior, and lateral views together with a sagittal section (left to right) of the fang showing different densities of mineralized tissues. A sharp and dense enameloid keel is present on the anterior edge; there is no comparable mineralized tissue along the posterior edge except distally in the region of the barb. Arrows marked B indicated the plane of the virtual dissection shown in (b). (b) Virtual dissection of the shaft of the fang showing vascular dentine and comparative density of mineralized tissues in the keel, barb, and tooth shaft. VIMS 35784, 1,034 mm TL, F

The pattern of replacement waves indicated by the dashed lines in Figure 10 can be understood in the context of alternate tooth replacement and the four-part staging system (A, I, F, E). In particular,

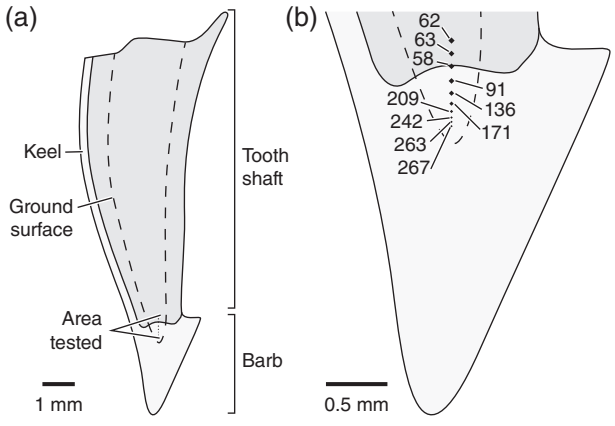

FIGURE 6 *Trichiurus lepturus* diamond indenter hardness testing of barb and tooth shaft of an epoxy embedded premaxillary fang. (a) Overview of fang showing region where measurements were made. (b) Close up showing positions of indentations and Vickers hardness (HV) values. Values for the enameloid of the barb ranged from 91 to 267 HV; dentine of the shaft was softer, with values ranging from 58 to 62 HV. VIMS 35784, 1,034 mm TL, F

a tooth locus scored as eroding would soon have lost its tooth and then be scored as absent. For example, there are three premaxillary waves in the specimen shown in Figure 10o. To understand how these three waves are coordinated, consider tooth loci 7, 9, 11, and 13. In the case of locus 9, the eroding tooth that was formerly there has been lost and thus locus 9 is scored as absent. Note that loci 7 and 11 are eroding. We interpret that a single eroding tooth in the middle of the first wave was lost at locus 9 because it eroded slightly faster than did the two adjacent loci (7 and 11) of the first wave. Similarly, the eroding tooth at locus 11 would soon have been lost, rendering this locus as absent. This would put locus 11 in complete alignment with the third tooth wave (i.e., loci 9, 13, 15, 17, and 19). Such variation in replacement waves reflects the biological reality and timing of tooth replacement across individuals.

The base lengths of lateral teeth increase toward the middle of the series of loci in both the premaxilla and dentary, and decrease from that point posteriorly (Figure 11a,b). A similar pattern occurs for tooth height (Figure 11a,b). The most posterior teeth in the series are smaller and slightly recurved (Figure 3b). Because the alveolar margin of the premaxilla is concave, the absolute height increase and subsequent decrease is not evident except from tooth measurements. All teeth have enameloid caps, but barbs only occur on dentary teeth on the widest and tallest teeth in the middle of the series; all lateral teeth

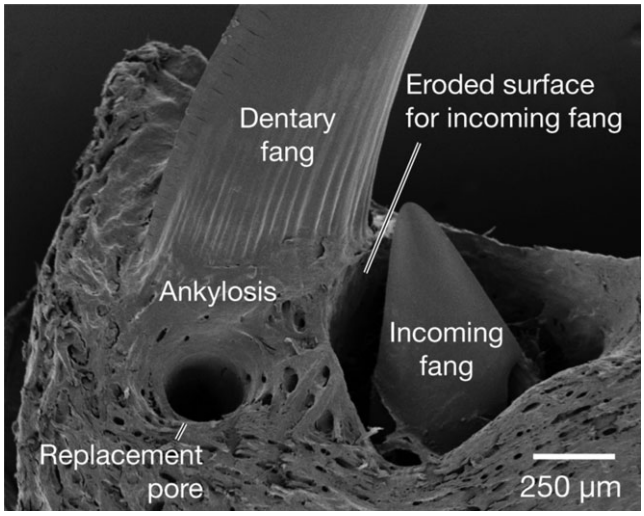

FIGURE 8 *Trichiurus lepturus*, scanning electron micrograph of fang and fang replacement at tip of left dentary. The functional fang is ankylosed to the bone and a replacement pore has developed at its base. An incoming fang immediately posterior to it is erupting through its replacement pore. Note the smooth edges of the replacement pore and smooth eroding surface surrounding the incoming fang. Anterior to left. VIMS 35776, 540 mm TL, M

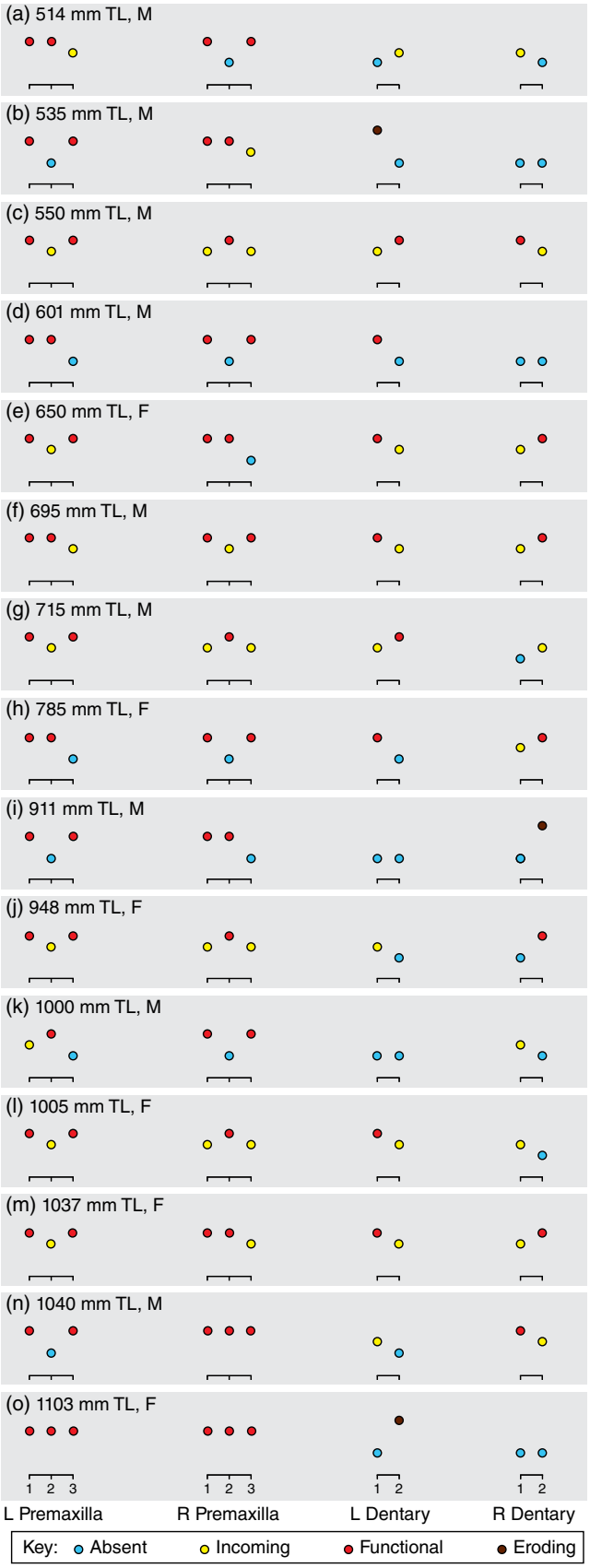

FIGURE 7 Condition of fangs at each locus in the left and right premaxilla, and left and right dentary for 15 individuals of *Trichiurus lepturus* arranged by TL scored as Absent, Incoming, Functional, or Eroding. Replacement status of the fang loci in the left ramus is often opposite to that in the right ramus when teeth are considered Ankylosed or Replacing. (a) VIMS 35770, 514 mm TL, M. (b) VIMS 35874, 535 mm TL, M. (c) VIMS 35769, 550 mm TL, M. (d) VIMS 35798, 601 mm TL, M. (e) VIMS 35774, 650 mm TL, F. (f) VIMS 35778, 695 mm TL, M. (g) VIMS 35777, 715 mm TL, M. (h) VIMS 35780, 785 mm TL, F. (i) VIMS 35791, 911 mm TL, M. (j) VIMS 35795, 948 mm TL, F. (k) VIMS 35790, 1,000 mm TL, M. (l) VIMS 35787, 1,005 mm TL, F. (m) VIMS 35788, 1,037 mm TL, F. (n) VIMS 35794, 1,040 mm TL, M. (o). VIMS 35779, 1,103 mm TL, F

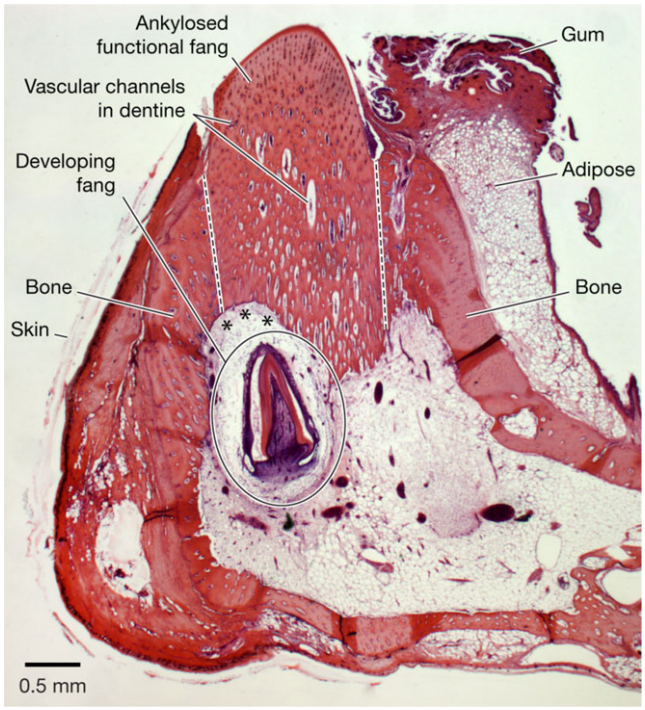

FIGURE 9 *Trichiurus lepturus*, histological section (6 μm) of dentary stained with hematoxylin and eosin showing a dentary fang developing directly beneath the ankylosed functional fang that it will replace. Dashed lines indicate the region of ankylosis between the vascular dentine of the fang and bone. Bone immediately adjacent to the dashed line is bone of attachment, which can be differentiated from the parallel-fibred bone of the dentary by its irregular vascular channels. Asterisks (*) indicate position of osteoclast resorption of dentine and bone to accommodate growth and eventual eruption of developing fang. Note the extremely thin skin surrounding the labial surface of the dentary. To the lingual side of the fang, a small pad of gum tissue is underlain by adipose. Due to plane of section, only one dentary locus and its replacement are visible in this image. VIMS 35894 (KEB2015-0060), 718 mm TL, F

of the premaxilla and lateral teeth at the anterior and posterior ends of the dentary lack barbs. Larvae and juvenile specimens examined lack barbed lateral teeth in the dentary, but have barbed premaxillary and dentary fangs. The number of barbed lateral teeth in the dentary increases as a function of TL (r^2 = .63; range = 0–8 barbs). The teeth of larger specimens are larger (Figure 11). Thus, over ontogeny, individuals increase both the number of loci and tooth size at a given locus. For example, in the specimen shown in Figure 11b, the eroding tooth at locus 11 indicated by an arrow is smaller in height and base length than the functional teeth adjacent to it in loci 10 and 12. This is because the adjacent functional teeth are from a later wave and thus larger than the eroding tooth between them.

Despite differences in tooth shape (e.g., barbed or not barbed), all lateral teeth in the premaxilla and dentary have the same replacement mode (Figures 10–14). For both the premaxilla and dentary, the numbers of Replacing Loci are approximately equal to those of Ankylosed Loci. In the 15 scored specimens, 573 premaxillary loci were scored: 51% were Replacing Loci and 49% were Ankylosed Loci. Of 717 dentary loci, 54% were Replacing Loci and 46% were Ankylosed Loci. There is no significant difference between the percentages of Replacing Loci and Ankylosed Loci in either the premaxilla or the dentary, and this indicates an almost perfectly alternate tooth replacement pattern across the entire sample. The alternate tooth replacement pattern is evident in most specimens, with I or A alternating with F or E teeth (Figure 12a).

Replacement waves for the lateral teeth in 15 specimens are indicated by dashed lines connecting loci in the same replacement wave (Figure 10). For example, in a 514 mm TL specimen (Figure 10a), there is a long replacement wave in the premaxilla consisting of five Absent Loci (1, 3, 5, 7, and 9), followed by two Incoming Loci (11 and 13), and two Functional Loci (15 and 17). A second replacement wave consists of six Functional Loci at positions 2, 4, 6, 8, 10, and 12. A third and very short replacement wave is indicated by Absent Loci 14 and 16. The oldest tooth in a given replacement wave is at its posteriormost locus. The number of replacement waves in the premaxilla ranged from 2 to 6 with a mode of 3 (Figure 10). The number of replacement waves in the dentary ranged from 3 to 7 with a mode of 4 (Figure 10).

Ankylosis is not complete until after an Incoming tooth erupts, but once the ankylosis develops, it is strong. For example, ankyloses at the bases of the fangs and lateral teeth (Figure 12a) are the densest tissues of the premaxilla. In the case of lateral teeth, incoming teeth develop within the bone, and erode bone of attachment (cone-shaped collars at the base of each functional tooth) as they erupt (Figure 12a). Constant processes of ankylosis and erosion remodel the jaws to accommodate tooth development, growth, and attachment. For example, the ankylosis of a functional tooth is eroded from both sides as new incoming teeth erupt; the ankyloses for the newly erupted teeth will not develop until later (Figure 12b).

Three waves of lateral teeth can be present at the same time. Near the top of the section shown in Figure 13, an Absent Locus is flanked by two Functional Loci. A new tooth germ, the youngest tooth, is migrating deep into the trench, passing between the two functional teeth and still connected to the oral epithelium by its dental lamina (Figure 13). Simultaneously, two developing teeth, intermediate in age between the tooth germ and the two functional teeth, have mineralized portions of the vascular dentine and keel but have not yet erupted. The two functional teeth, which are the first wave shown, would soon have been lost. The two developing teeth that are part of the second wave would have erupted into the Absent Loci adjacent to the Functional Loci. The tooth germ, which is the third wave visible, would have continued to sink beneath the functional tooth to its left, and developed to eventually replace it.

Unlike the obvious replacement pores for premaxillary and dentary fangs, the replacement pores for lateral teeth are harder to define. Because the new tooth germ and the incoming tooth together erode bony tissues at an Absent Locus between ankylosed teeth, there is extensive and continuous remodeling of bone around each replacement pore in the trench (Figures 4b, 12b, and 13).

3.4 | Phylogenetic comparisons

We examined tooth replacement patterns in scombroids (see Appendix) and highlight several specific comparisons here using Figure 14.

Pomatomidae. The Bluefish, *Pomatomus saltatrix*, lacks fangs in both the premaxilla and dentary fangs (Figure 14a). Tooth replacement is alternate throughout the jaw (Bemis et al., 2005). New tooth

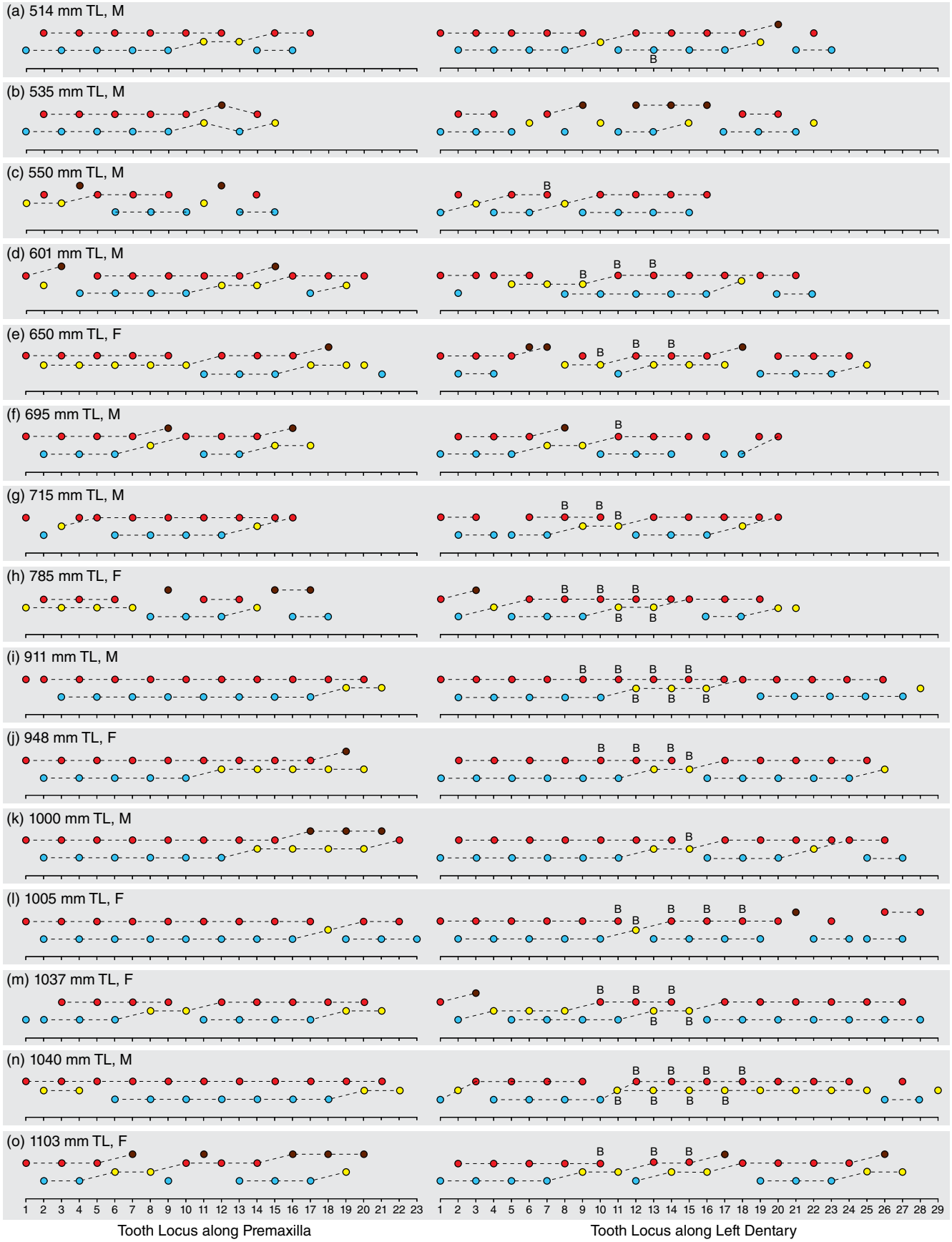

FIGURE 10. Legend on next page.

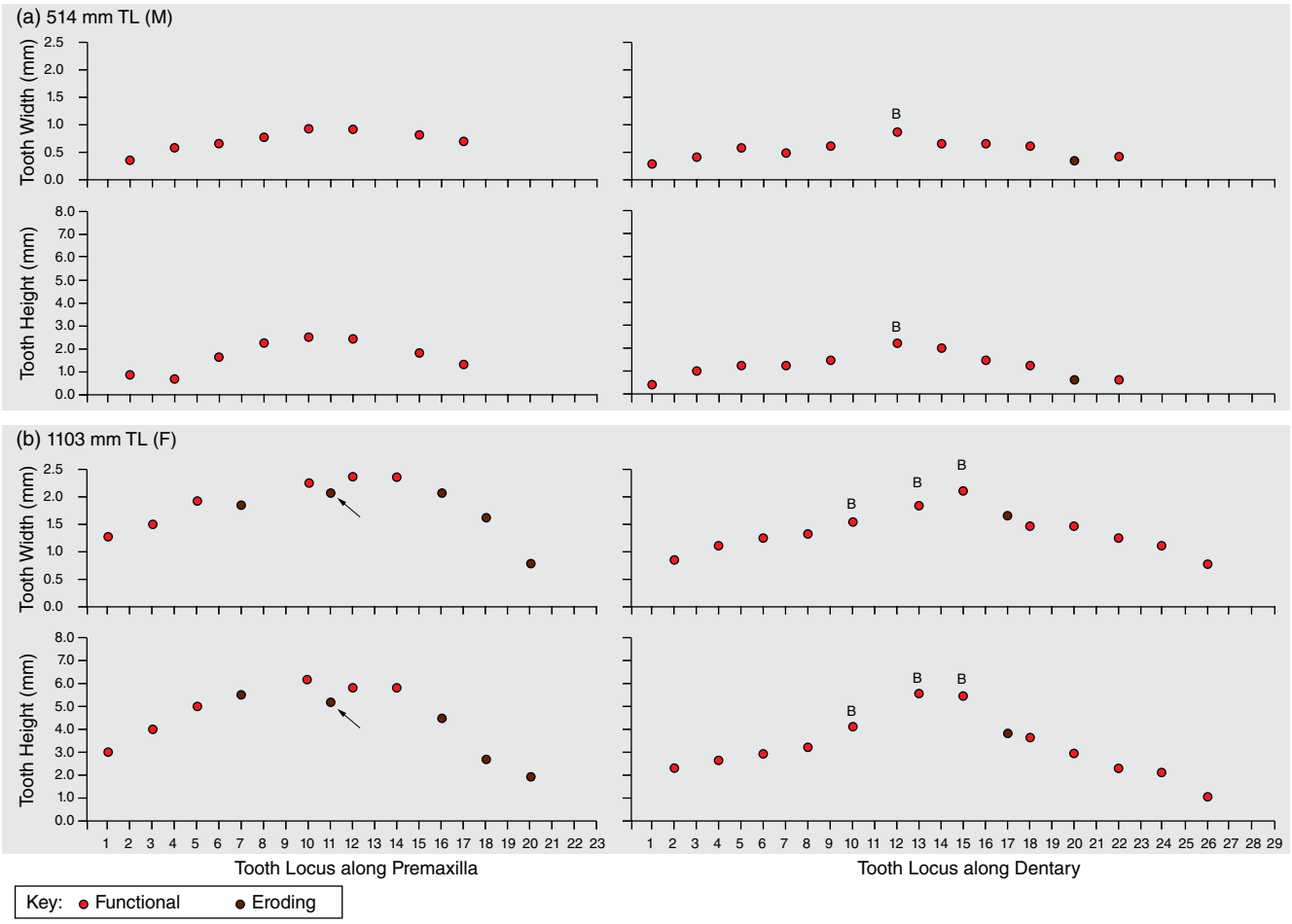

FIGURE 11 Dimensions of teeth in left premaxilla and dentary in two specimens of *Trichiurus lepturus*. Tooth base length and tooth height are expressed as a function of locus number. Only two stages of teeth are shown (functional in red and eroding in brown) because it is not possible to accurately measure Absent or Incoming loci. Arrow indicates an eroding tooth at locus 11 from a previous wave that is smaller than the subsequent wave of functional teeth at its flanking loci 10 and 12. The presence of barbs on teeth is indicated with B. (a) VIMS 35769, 514 mm TL, M. (b) VIMS 35779, 1,103 mm TL, F

germs for the teeth of *P. saltatrix* migrate into the dentigerous bone via replacement pores on the labial side of the premaxilla and the lingual side of the dentary as opposed to entering via a trench (Figure 14a). In the case of *P. saltatrix*, a replacement pore is largest just after it has admitted a tooth germ into the dentigerous bone. This is because the tooth germ migrates through the enlarged pore to reach its position directly underneath the tooth that it will replace. Subsequently, the replacement pore becomes smaller. The new tooth germ that entered the jaw continues to develop below the older tooth that it will replace, and as it grows, it enters the older tooth's pulp cavity. There is a pattern of replacement pore sizes in relation to the tooth condition (A, I, F, or E) at each locus along the jaw. Large replacement pores are associated with Functional teeth and small pores with Absent Loci; a pore may close completely after the tooth germ has migrated into the jaw. The large pores are the youngest because a tooth germ has just entered through the pore; the pore will eventually be closed over as the surrounding bone is remodeled. A new tooth of *P. saltatrix* does not erupt through its replacement pore (Bemis et al., 2005). In contrast, replacement pores remain open in all three replacement modes in *Trichiurus lepturus*, and new teeth erupt through them.

Scombrolabracidae. Scombrolabrax heterolepis has distinctive premaxillary and dentary fangs (Figure 14b). The fangs develop in loci that we presume to be homologous to the fang loci of *Trichiurus lepturus* because the replacement pores are on the lingual side of the premaxilla, and the labial side of the dentary. The premaxillary fangs develop

FIGURE 10 Condition of lateral teeth of *Trichiurus lepturus* at each locus in the left premaxilla and left dentary scored as Absent, Incoming, Functional, or Eroding for 15 individuals arranged by TL. Dashed lines connect loci within a replacement wave. Data for the premaxilla are shown on the left side, and corresponding data for dentary are shown on the right. Dentary teeth bearing barbs indicated with B. (a) VIMS 35770, 514 mm TL, M. (b) VIMS 35874, 535 mm TL, M. (c) VIMS 35769, 550 mm TL, M. (d) VIMS 35798, 601 mm TL, M. (e) VIMS 35774, 650 mm TL, F. (f) VIMS 35778, 695 mm TL, M. (g) VIMS 35777, 715 mm TL, M. (h) VIMS 35780, 785 mm TL, F. (i) VIMS 35791, 911 mm TL, M. (j) VIMS 35795, 948 mm TL, F. (k) VIMS 35790, 1,000 mm TL, M. (l) VIMS 35787, 1,005 mm TL, F. (m) VIMS 35788, 1,037 mm TL, F. (n) VIMS 35794, 1,040 mm TL, M. (o) VIMS 35779, 1,103 mm TL, F

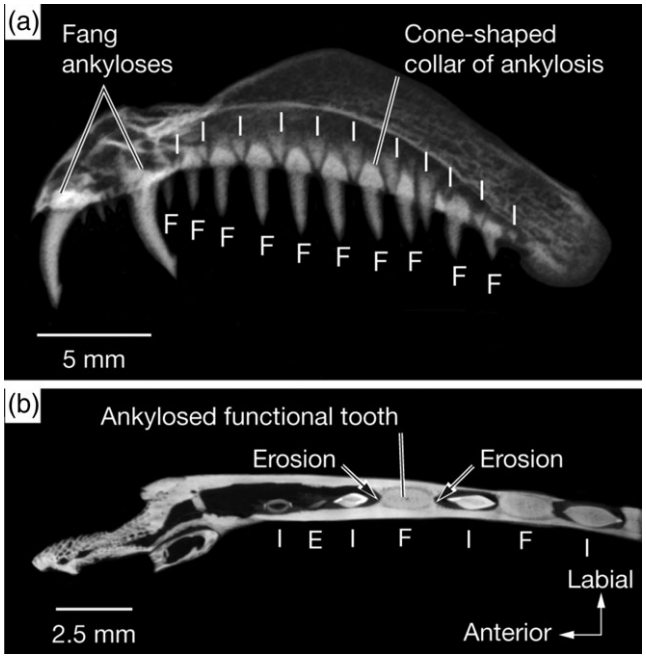

FIGURE 12 *Trichiurus lepturus*, X-ray views of ankylosis and erosion of teeth and bone. (a) Conventional X-ray of right premaxilla viewed from lingual surface showing alternate tooth replacement of lateral teeth with Incoming Loci (I) located between Functional Loci (F). Note the dense ankylosis of two premaxillary fangs and the cone shaped collars of the bone of attachment surrounding the bases of the functional lateral teeth, which ankylose the teeth to the dentigerous bone. VIMS 35787, 1,005 mm TL, F. (b) Frontal section of right premaxilla reconstructed from CT data set to show ankylosis and erosion in relation to a functional tooth. The indicated tooth is ankylosed to the premaxilla, and, flanking it, are two incoming teeth not yet ankylosed. Erosion occurs to allow the incoming tooth to erupt. VIMS 35776, 540 mm TL, M

vertically and do not rotate into place. Pores for dentary fangs are located more anteriorly and ventrally than in *T. lepturus*, and dentary fangs erupt vertically. Like *T. lepturus*, the lateral teeth of *S. heterolepis* replace via a trench. Tooth replacement is alternate throughout the jaws.

Trichiuridae + "Gempylidae." Other trichiurids and "gempylids" (Figure 14c; Appendix) show patterns of tooth replacement similar to *Trichiurus lepturus*. The 2–3 premaxillary fangs on each ramus develop horizontally from replacement pores located on the lingual surface of the premaxilla; all three replacement modes are present. *Gempylus serpens* (Figure 14c) has a remarkably similar dentition and replacement pattern to that of *T. lepturus*; the incoming fangs can be depressed with a probe before they ankylose to the bone. There are two loci for dentary fangs, which develop through replacement pores on the labial surface; new dentary fangs erupt vertically without rotating. Lateral teeth of the premaxillae and dentaries develop in trenches as in *T. lepturus*. Tooth replacement is alternate in all three modes. In some "gempylids" with smaller fangs, like *Promethichthys prometheus*, premaxillary fang development rotation is present, but the rotation is less extreme.

Scombridae. Scombrid teeth vary greatly in size and shape, but all taxa examined lack premaxillary and dentary fangs (Figure 14d; Appendix). The teeth of scombrids are replaced in a trench, using the same mode that we observed for the lateral teeth of *Trichiurus lepturus*. Replacement is alternate. The teeth of *Scomber scombrus* are among the smallest teeth examined in this survey; however, they exhibit typical alternate replacement. There are no replacement pores on the labial or lingual surfaces.

4 | DISCUSSION

Although age and growth of *Trichiurus lepturus* have been studied in other regions (e.g., Kwok & Ni, 2000, South China Sea), comparable data do not exist for the western North Atlantic population. Such information would inform estimates of absolute rates of tooth replacement because more teeth are added as a fish grows. We infer from the strongly alternate replacement pattern that tooth replacement is closely regulated, with teeth replaced on a schedule rather than as they are damaged. A higher percentage of the ankylosed teeth are functional rather than eroding, which suggests that individual teeth are quickly lost once erosion begins but that teeth remain functional for extended periods of time. A similar interpretation was suggested for two other scombroids, *Scomberomorus cavalla* (Morgan & King, 1983: fig. 1) and *Pomatomus saltatrix* (Bemis et al., 2005: fig. 5).

The premaxillary fangs, dentary fangs, and barbed lateral teeth of *Trichiurus lepturus* have cutting edges along the keel and the posterior edge of the barb (Figure 5). Unbarbed lateral teeth are compressed, with cutting edges on both the anterior and posterior surfaces of the tooth. CT scans and hardness testing (Figures 5 and 6) show that the barb and keel are much harder than the dentine of the shaft. The average Vickers hardness for the barb tip is 213 HV ($SD \pm 44$; Figure 6), somewhat lower than that of mammalian enamel (>270 HV for humans; Gutiérrez-Salazar & Reyes-Gasga, 2003). The average Vickers hardness for the tooth shaft is 53 HV ($SD \pm 3$), comparable to mammalian dentine (50–60 HV for humans, Gutiérrez-Salazar & Reyes-Gasga, 2003). Hardening and reinforcement of cutting edges and barbs likely have functional implications for capturing and processing prey. There are no detailed studies on feeding behavior of *T. lepturus*, but Martins et al. (2005) reported field observations of feeding by large *T. lepturus* suggesting that they impale and cut prey items. These authors also reported ontogenetic shifts in diet: larvae (<5 cm) feed primary on calanoid copepods, juveniles (5–30 cm) feed on small zooplanktonic crustaceans, subadults (30–70 cm) feed on euphausiids and small fishes like anchovies, and large adults (70–160 cm) cannibalize other *T. lepturus*, feed on sciaenids, cephalopods, and shrimps, as well as anchovies and euphausiids. Despite these ontogenetic changes in diet, barbed and keeled teeth are present in larval *T. lepturus*. De Schepper, Wassenbergh, and Adriaens (2008) suggested that rapid closing of the jaws and a powerful bite help to ensure prey capture; their study documented both attributes in *T. lepturus*. Long jaws facilitate rapid closing and increased gape, which allows *T. lepturus* to capture large prey (De Schepper et al., 2008).

We found three modes of tooth replacement in *Trichiurus lepturus* related to the location of the tooth locus in the jaw (Figure 15). Mode 1 relates to replacement of premaxillary fangs via horizontal development of replacement fangs and rotation into place before ankylosis; the replacement pores are located on the lingual surface of the premaxilla. In Mode 2, dentary fangs develop from tooth germs that enter replacement pores on the labial surface of the dentary, migrate deeply beneath the functional tooth, develop vertically, and erupt directly

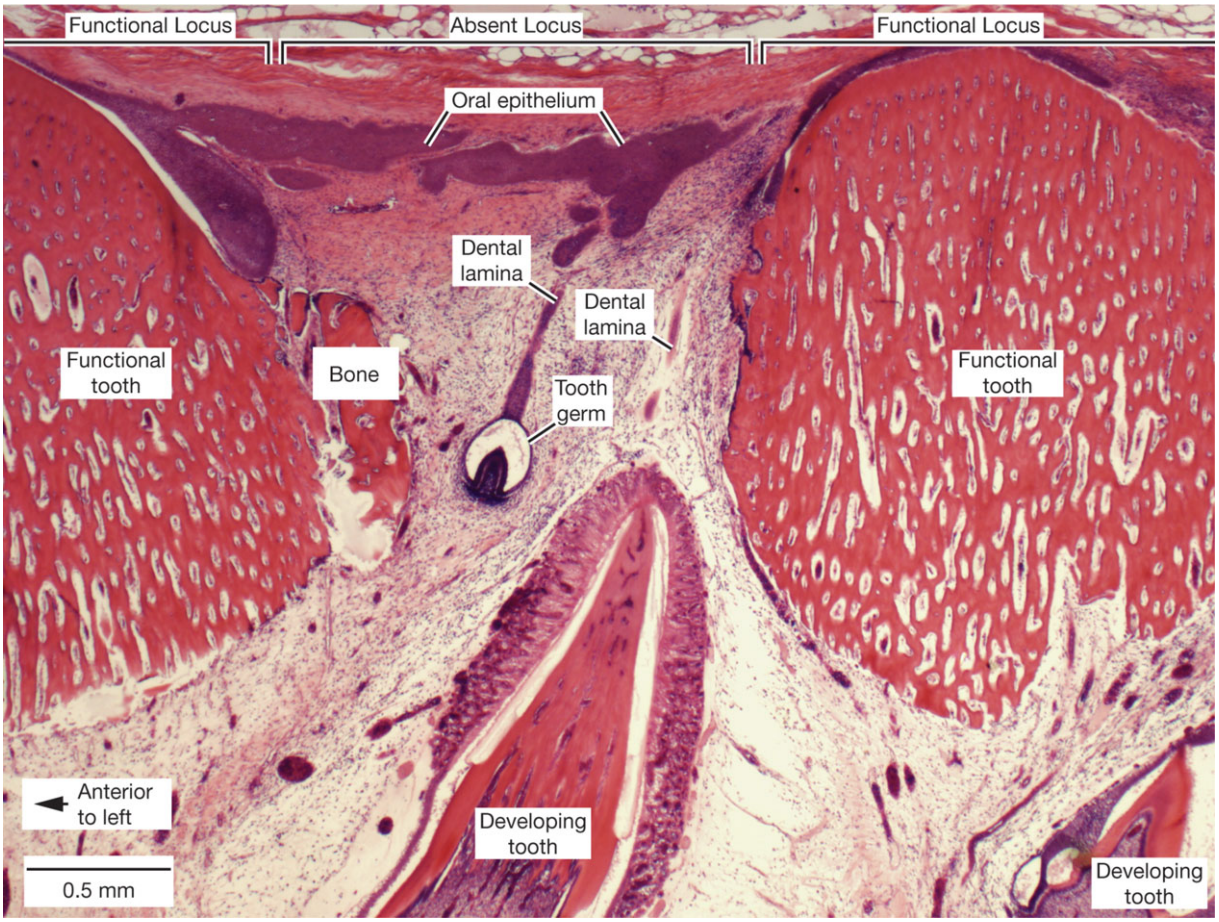

FIGURE 13 *Trichiurus lepturus*, histological section (6 μm) of dentary stained with hematoxylin and eosin showing three waves of teeth. Two functional teeth, ankylosed to adjacent bone, flank an Absent Locus. A new tooth germ, still connected to the oral epithelium by its dental lamina, migrates deeply into the jaw between the two functional teeth. Simultaneously, a developing tooth is positioned to erupt through the same opening; traces of its dental lamina are present. Note the enameloid cap of the developing tooth. VIMS 35894 (KEB2015-0060), 718 mm TL, F

into position before ankylosis. Lateral teeth develop via Mode 3: new tooth germs form in soft tissues in a trench along the crest of the dentigerous bone and then migrate into the bone between adjacent Functional Loci (Figure 13). The tooth germs of lateral teeth develop vertically beneath existing teeth and erupt directly into position before ankylosis. In all three modes, tooth replacement is alternate and very strong ankyloses develop. We found no reports that document such distinctly different modes of tooth replacement in one species of teleost (e.g., Berkovitz & Shellis, 2017).

We surveyed 20 species of scombroids (Figure 14; Appendix) to explore the phylogenetic distribution of the three tooth replacement modes found in *Trichiurus lepturus* (Figure 16). Orrell et al. (2006) placed *Pomatomus saltatrix* at the base of Scombroidei, and it shares many features of tooth replacement with other scombroids (e.g., alternate tooth replacement, strong ankyloses of teeth, and intraosseous tooth replacement; Bemis et al., 2005; Johnson, 1986). However, these features occur in many other percomorph taxa and are likely plesiomorphic to Scombroidei (Figure 16). *Scombrolabrax heterolepis* has premaxillary and dentary fangs, so we can compare all three replacement modes to those observed in *T. lepturus*. A key difference is that the relatively shorter premaxillary fangs of *S. heterolepis* do not rotate during their development. In *T. lepturus* and *Gempylus serpens*, all three tooth replacement modes are present and very similar. In *Scomber scombrus*, however, premaxillary and dentary fangs are absent, meaning that only replacement Mode 3 occurs. Key differences among the taxa summarized in Figure 16 include the opposite location of replacement pores in *P. saltatrix* compared to the fang pores of *S. heterolepis*, *T. lepturus*, and *G. serpens*; rotation of the premaxillary fangs in *T. lepturus* and *G. serpens*; and the absence of fangs in *S. scombrus*, which we interpret as a phylogenetic loss. Although there is great variation in the dentitions of scombroids, such as the shapes and details of the teeth (e.g., size, keels, barbs, serrations, and so forth), the replacement modes, especially within clades, are conserved.

4.1 | Dental lamina and replacement pores

The source of epithelial cells for new tooth formation can either be from the preceding generation of teeth, a condition known as a successional dental lamina (Huysseune, 2006), or the epithelium can enter directly through replacement pores that extend the dental lamina from its initial site in the oral epithelium (Bemis et al., 2005; Thiery et al., 2017). Huysseune (2006) described a successional dental lamina in the pharyngeal jaw of *Danio rerio*, which has extraosseous tooth replacement, in which a new tooth germ is derived in part from the epithelium of a predecessor tooth, that is, there is an epithelial strand connecting the new tooth germ with its predecessor. Such a successional dental lamina occurs when the

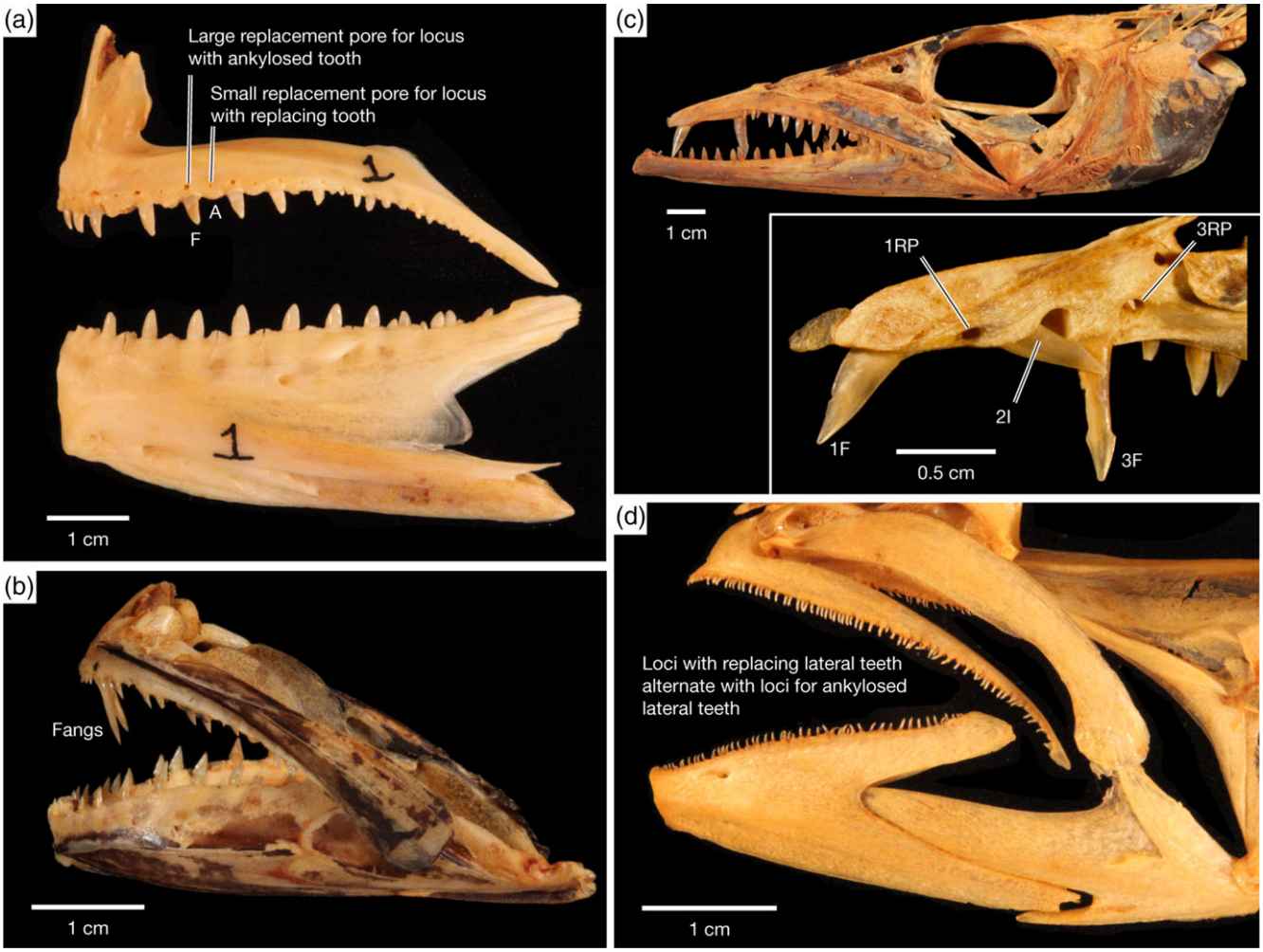

FIGURE 14 Comparisons of teeth and tooth replacement in scombroids (sensu Orrell et al., 2006). All four of these taxa exhibit alternate tooth replacement in the oral jaws. (a) *Pomatomus saltatrix*: The large teeth of the dentary and premaxilla are homodont and no fangs are present. Replacement pores for the premaxilla are on the labial side; those for the dentary are on the lingual side. In both cases, large replacement pores are beneath ankylosed teeth. Small pores, if present, are beneath replacing teeth. CUMV 97588. (b) *Scombrolabrax heterolepis*: a single pair of premaxillary fangs is present; dentary fangs are present but small (not visible in this photograph). The lateral teeth are similar to those of *Trichiurus* and replace via a trench. AMNH 211557, est. 200 mm SL. (c) *Gempylus serpens*: Three premaxillary fang loci and two dentary fang loci are present as in *Trichiurus* and the replacement modes are similar to those of *Trichiurus*. The lateral teeth replace via a trench. Skull of AMNH 90898; inset showing lingual view of right premaxilla of AMNH 90897. (d) *Scomber scombrus*: no fangs are present and all teeth are replaced via a trench. AMNH 55859, est. 355 mm SL

new tooth germ is part of an established tooth family (Huysseune, 2006). In contrast, the dental lamina in *Trichiurus lepturus* derives directly from the oral epithelium and is not connected to that of a predecessor tooth. We term this a direct dental lamina to distinguish it from the successional lamina described by Huysseune (2006). Such a direct dental lamina occurs in other species with intraosseous tooth replacement in the oral jaws (e.g., Bemis et al., 2005; Bemis & Bemis, 2015; Thiery et al., 2017) although this is our first use of the term direct dental lamina. We think that characters related to the type of tooth replacement (extraosseous vs. intraosseous), the position of the dental lamina (successional vs. direct), the occurrence of replacement pores (present or absent), and the position of replacement pores (lingual side, labial side, or crest of dentigerous bone) have phylogenetic signals. Until more taxa are surveyed, however, it is not possible to establish whether the direct dental lamina is part of a character complex linked to intraosseous tooth development or whether it should be interpreted as a separate character.

4.2 | Coupling of tooth formation and bone erosion processes

The locations where tooth germs enter the bone influence subsequent developmental processes related to bone erosion and remodeling, and, by extension, are directly related to functional anatomical considerations such as the strength of the dentigerous bones. By eroding into the side of the dentigerous bone, a tooth germ of *Pomatomus saltatrix* invades directly into the base of the functional tooth (and eventually its pulp cavity) that it will replace. This process links new tooth formation to erosion of the old tooth (Bemis et al., 2005: figs. 9 and 10). In contrast, tooth germs for the lateral teeth of *Trichiurus lepturus* erode into bone from the trench along the crest of the dentigerous bone in association with an Absent Locus. Simultaneously, a developing tooth nears eruption into that locus (Figure 13). Such coupling of tooth germ entry and

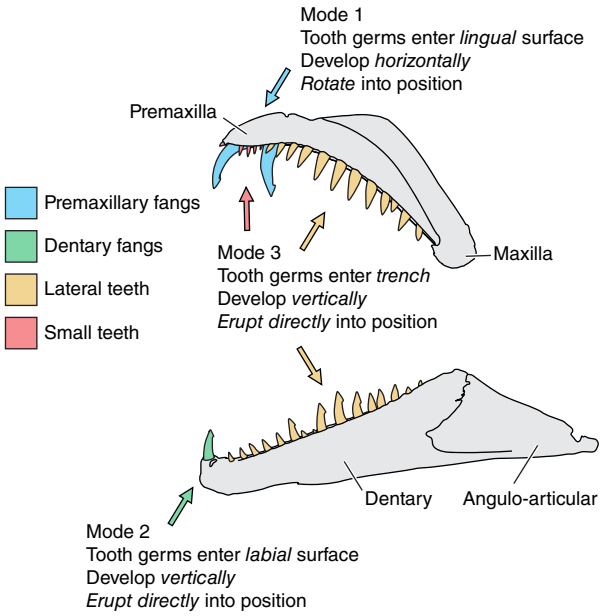

FIGURE 15 Summary of the three modes of tooth replacement in *Trichiurus lepturus*

eruption minimizes bone erosion, and allows a passage for the incoming tooth. As a result, much of the bone eroded during lateral tooth germ migration of *T. lepturus* is bone of attachment, not the parallel-fibred bone (Francillon-Vieillot et al, 1990) through which the tooth germs of *P. saltatrix* pass. In both cases, erosion depends on osteoclasts, but the patterns of development are different. Differences between the Bluefish Type and Cutlassfish Type of tooth replacement (Figure 17) are not simply the result of moving the site of origin of tooth germs because the mechanisms by which tooth germs enter the bone are coupled to subsequent developmental processes of bone erosion, remodeling, and tooth ankylosis. The differences between *P. saltatrix* and *T. lepturus* show that there are multiple ways for intraosseous tooth replacement to yield alternate tooth replacement with strong ankyloses of teeth.

4.3 | Evolution of intraosseous replacement in *Trichiurus lepturus*

Developing tooth germs can be protected from potential damage during feeding by soft tissues and/or bone (Morgan, 1977). In the case of *Trichiurus lepturus*, the skin and oral mucosa are too thin to offer much protection to tooth germs (Figure 8a). Tooth germs developing in a trench are better protected than they would be if they entered the bone on either its lingual or labial side. In the case of the premaxillary fangs, horizontal replacement may protect large teeth as they develop, but it is also possible that such horizontal development is related to space constraints. The jaws of *T. lepturus* are thin and lightly built of parallel-fibred

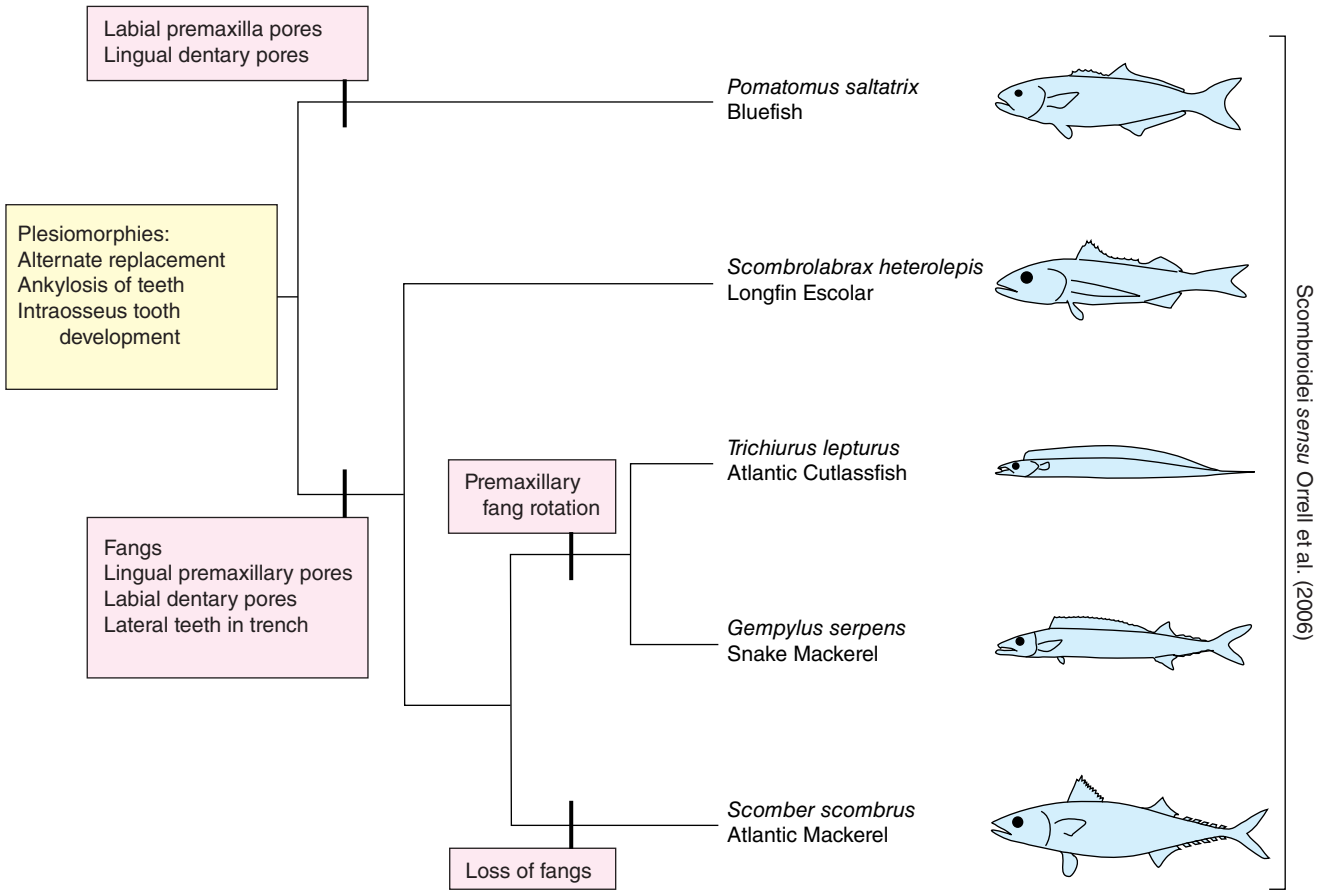

FIGURE 16 Simplified phylogeny for Scombroidei based on Orrell et al. (2006), highlighting differences in tooth development in Bluefish + other scombroids. Derived features that are putative synapomorphies are indicated in pink boxes. Symplesiomorphies are indicated at the base in a yellow box

bone. More bone is present near the premaxillary symphysis, but it is still insufficient to allow vertical development of elongate fangs, particularly because there are three fang loci in this compact region. Perhaps the small overall height of the premaxilla relative to its long fangs constrains fang development. If so, then rotational fang development is a mechanism for developing large premaxillary fangs. Dentary fangs develop vertically: they are shorter than premaxillary fangs, and there are only two loci, so there is more space and better protection for developing fangs within the bone prior to their eruption.

Although yet to be formally surveyed, we have observed horizontal rotation during replacement of large fangs in other families of teleosts such as Cynodontidae (intraosseous) and Alepisauridae (extraosseous). Horizontal tooth development and rotation into the functional position also occurs in snakes. For example, replacement teeth in the lower jaw of the Rhinoceros Horned Viper (*Bitis nasicornis*) develop in a horizontal position; the new teeth rotate on eruption into the functional position before ankylosis (Berkovitz & Shellis, 2017: fig. 7.21). A similar replacement mode occurs in elapid snakes (Berkovitz & Shellis, 2017, p. 216). Rotational development of teeth in snakes convergently resembles the condition in Alepisauridae because in both taxa tooth development is extraosseous.

Replacement premaxillary fangs of trichiurids and "gempylids" have been misinterpreted in some taxonomic works, with incoming fangs described as "depressible teeth" (e.g., Ho, Motomura, Hata, & Jiang, 2017; Tucker, 1956). These teeth are merely a stage (incoming) during the development of premaxillary fangs. The number of incoming premaxillary fangs varies over time and needs to be viewed in the context of tooth replacement overall.

Intraosseous tooth replacement is a complex and variable process that has evolved repeatedly within teleosts. Key processes include the sites of formation of new tooth germs and points of entry into bones, whether teeth develop horizontally or immediately beneath the tooth that they will replace, and how erosion, tooth eruption, and ankylosis occur. These processes can differ, but still yield similar dentitions (Figure 17). In the modes of tooth replacement described to date, details vary, and the full implications of such differences remain unexplained. Further descriptions of the diversity of tooth replacement modes of teleosts will contribute to a better understanding of phylogenetic patterns as well as the functional anatomy and development of teeth.

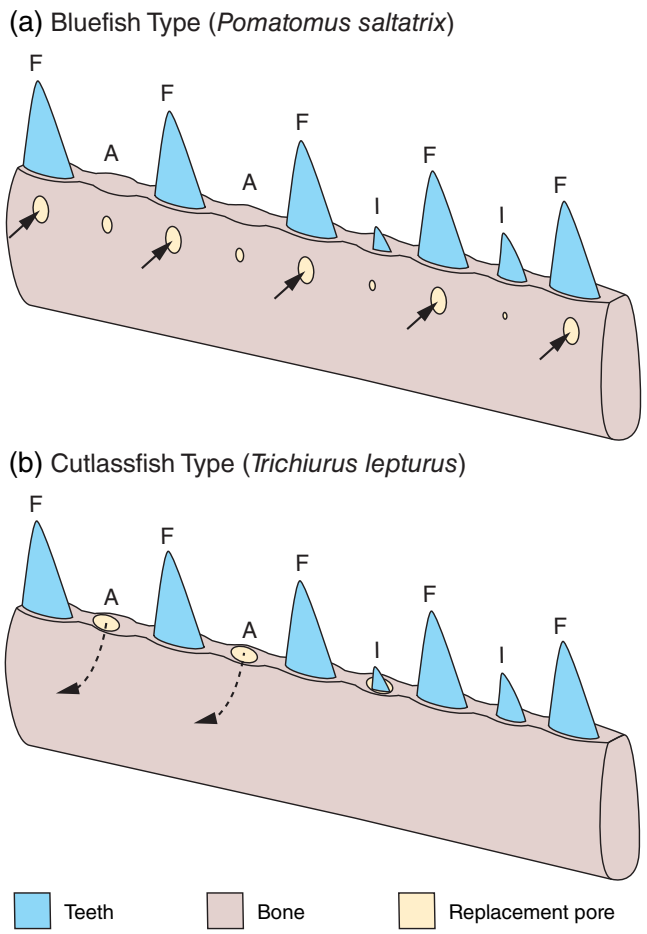

FIGURE 17 Two types of tooth replacement exemplified by (a) Bluefish (*Pomatomus saltatrix*) and (b) Atlantic Cutlassfish (*Trichiurus lepturus*). Arrows indicate locations where tooth germs enter the bone; dotted lines indicate path of the tooth germ within the bone. Both types couple bone erosion and deposition in highly dynamic processes. Key differences relate to the position of the replacement pores and the migration pathway of tooth germs once they enter the bone, which affects how erosion proceeds

ACKNOWLEDGMENTS

We thank J. Galbraith, H. Cook, and J. Kircun of the Northeast Fisheries Science Center (NEFSC) who collected many of the specimens examined, and we are grateful for the wealth of specimens and information available from the NEFSC Ecosystems Survey Branch. We thank T. Hughes, C. Copeland, and C. Fox for help preparing skeletal material. We thank S. Huber, VIMS, for cataloging and curating new specimens collected for this project, and the following individuals for loans of comparative material: D. McElroy, NEFSC; C. Dardia, CUMV; T. Cullins, SEAMAP and L. Habegger, Florida Southern College; R. Arrindale, B. Brown, and T. Vigliotta, AMNH; M. Arce and M. Sabaj, ASNP; K. Murphy and S. Raredon, USNM. A. S. Martins provided valuable information about cutlassfish diet. M. Riccio and T. Porri, Cornell University Biotechnology Resource Center, performed CT scans. W. Allmon, Paleontological Research Institution, provided access to SEM facilities. We also thank M. Slade, Cornell Veterinary College Diagnostic Laboratory, and P. Carubia of Cornell Center for Materials Research (facilities supported by NSF MRSEC program, DMR-1120296). B. Collette, N. Schnell, and M. Vecchione reviewed an earlier version of the article, and L. Schaffner and C. Cake provided writing support. Research support provided by NSF Graduate Research Fellowship Program, VIMS Foundation Nancy S. and Henry George Fellowship, Cornell University Jane E. Brody Undergraduate Research Grant, Morley Student Research Grant, and Tontogany Creek Fund. This paper is Contribution No. 3787 of the Virginia Institute of Marine Science, College of William & Mary.

ORCID

Katherine E. Bemis https://orcid.org/0000-0002-7471-9283

REFERENCES

Beckett, H. T., Giles, S., Johanson, Z., & Friedman, M. (2018). Morphology and phylogenetic relationships of fossil snake mackerels and cutlassfishes (Trichiuroidea) from the Eocene (Ypressian) London Clay Formation. *Papers in Paleontology*, 1–27. https://doi.org/10.1002/spp2.1221

Bemis, K. E., & Bemis, W. E. (2015). Functional and developmental morphology of tooth replacement in the Atlantic Wolffish, *Anarhichas lupus* (Teleostei: Zoarcoidei: Anarhichadidae). *Copeia*, *103*(4), 886–901. https://doi.org/10.1643/OT-14-141

Bemis, W. E. (1984). Morphology and growth of lepidosirenid lungfish tooth plates (Pisces: Dipnoi). *Journal of Morphology*, *179*, 73–93. https://doi.org/10.1002/jmor.1051790108

Bemis, W. E., Giuliano, A., & McGuire, B. (2005). Structure, attachment, replacement and growth of teeth in Bluefish, *Pomatomus saltatrix* (Linnaeus, 1766), a teleost with deeply socketed teeth. *Zoology*, *108*, 317–327. https://doi.org/10.1016/j.zool.2005.09.004

Bemis, W. E., Hilton, E. J., Brown, B., Arrindell, R., Richmond, A. M., Little, C. D., … Nelson, G. J. (2004). Methods for preparing dry, partially articulated skeletons of osteichthyans, with notes on making Ridewood dissections of the cranial skeleton. *Copeia*, *2004*(3), 603–609. https://doi.org/10.1643/CI-03-054R1

Berkovitz, B., & Shellis, P. (2017). *The teeth of non-mammalian vertebrates*. Amsterdam, the Netherlands: Elsevier.

Betancur-R, R., Wiley, E. O., Arratia, G., Acero, A., Bailly, N., Miya, M., … Ortí, G. (2017). Phylogenetic classification of bony fishes. *BMC Evolutionary Biology*, *17*(162), 1–40. https://doi.org/10.1186/s12862-017-0958-3.

Conway, K. W., Bertrand, N. G., Browning, Z., Lancon, T. W., & Clubb, F. J., Jr. (2015). Heterodonty in the New World: An SEM investigation of oral dentition in the clingfishes of the subfamily Gobiesocinae (Teleostei: Gobiesocidae). *Copeia*, *103*(4), 973–998. https://doi.org/10.1643/OT-15-234

De Schepper, N., Wassenbergh, S. V., & Adriaens, D. (2008). Morphology of the jaw system in trichiurids: Trade-offs between mouth closing and biting performance. *Zoological Journal of the Linnean Society*, *152*, 717–736. https://doi.org/10.1111/j.1096-3642.2008.00348.x

Fink, W. L. (1981). Ontogeny and phylogeny of tooth attachment modes in actinopterygian fishes. *Journal of Morphology*, *167*, 167–184.

Francillon-Vieillot, H., de Buffrénil, V., Castanet, J., Géraudie, J., Meunier, F. J., Sire, J. Y., … de Riclès, A. (1990). Microstructure and mineralization of vertebrate skeletal tissues. In J. G. Carter (Ed.), *Skeletal biomineralization: Patterns, processes and evolutionary trends* (pp. 471–530). New York, NY: Van Nostrand Reinhold.

Grande, L. (2010). An empirical synthetic pattern study of gars (Lepisosteiformes) and closely related species, based mostly on skeletal anatomy. The resurrection of Holostei. *Copeia, ASIH Special Publication 6, 2010*, 1–871.

Gutiérrez-Salazar, M. P., & Reyes-Gasga, J. (2003). Microhardness and chemical composition of human tooth. *Materials Research*, *6*, 367–373. https://doi.org/10.1590/S1516-14392003000300011

Hall, B. K. (2015). *Bones and cartilage: Developmental and evolutionary skeletal biology* (2nd ed.). Amsterdam, the Netherlands: Academic Press.

Ho, H.-C., Motomura, H., Hata, H., & Jiang, W.-C. (2017). Review of the fish genus *Epinnula* Poey (Perciformes: Gempylidae), with description of a new species from the Pacific Ocean. *Zootaxa*, *4363*(3), 393–408. https://doi.org/10.11646/zootaxa.4363.3.5

Humason, G. L. (1972). *Animal tissue techniques*. San Francisco, CA: W. H. Freeman.

Huysseune, A. (2006). Formation of a successional dental lamina in the zebrafish (*Danio rerio*): Support for a local control of replacement tooth initiation. *International Journal of Developmental Biology*, *50*, 637–643.

Huysseune, A., & Witten, P. E. (2006). Developmental mechanisms underlying tooth patterning in continuously replacing osteichthyan dentitions. *Journal of Experimental Zoology*, *306B*, 204–215. https://doi.org/10.1002/jez.b.21091

Johnson, G. D. (1986). Scombroid phylogeny: An alternative hypothesis. *Bulletin of Marine Science*, *39*(1), 1–41.

Kwok, K. Y., & Ni, I.-H. (2000). Age and growth of cutlassfishes, *Trichiurus* spp., from the South China Sea. *Fishery Bulletin*, *98*(4), 748–758.

Martins, A. S., Haimovici, M. M., & Palacios, R. (2005). Diet and feeding of the cutlassfish *Trichiurus lepturus* in the subtropical convergence ecosystem of southern Brazil. *Journal of the Marine Biological Association of the United Kingdom*, *85*, 1223–1229.

Melo, M. R. S. (2009). Revision of the genus *Chiasmodon* (Acanthomorpha: Chiasmodontidae), with the description of two new species. *Copeia*, *2009*(3), 583–608. https://doi.org/10.1643/CI-08-048

Miya, M., Friedman, M., Satoh, T. P., Takeshima, H., Sado, T., Iwasaki, W., … Nishida, M. (2013). Evolutionary origin of the Scombridae (tunas and mackerels): Members of a Paleogene adaptive radiation with 14 other pelagic fish families. *PLoS One*, *8*(9), e73535. https://doi.org/10.1371/journal.pone.0073535

Morgan, E. C. (1977). Dentitional phenomena and tooth replacement in the scabbard fish *Trichiurus lepturus* Linnaeus (Pisces: Trichiuridae). *Texas Journal of Science*, *29*, 71–77.

Morgan, E. C., & King, W. K. (1983). Tooth replacement in king mackerel, *Scomberomorus cavalla* (Pisces: Scombridae). *The Southwestern Naturalist*, *28*(3), 261–269.

Nakamura, I., & Parin, N. V. (1993). *Snake mackerels and cutlassfishes of the world (Families Gempylidae and Trichiuridae): An annotated and illustrated catalogue of the snake mackerels, snoeks, escolars, gemfishes, sackfishes, domine, oilfish, cutlassfish, hairtails and frostfishes known to date FAO species catalogue* (Vol. 15). Rome, Italy: Food and Agriculture Organization.

Orrell, T. M., Collette, B. B., & Johnson, G. D. (2006). Molecular data support separate scombroid and xiphioid clades. *Bulletin of Marine Science*, *79*(3), 505–519.

Politis, P. J., Galbraith, J. K., Kostovick, P., & Brown, R. W. (2014). Northeast Fisheries Science Center bottom trawl survey protocols for the NOAA Ship Henry B. Bigelow. US Department of Commerce, Northeast Fish Sciences Center Reference Document 14-06; 138 p. Retrieved from http://nefsc.noaa.gov/publications/

Rosset, A., Spadola, L., & Ratib, O. (2004). OsiriX: An open-source software for navigating in multidimensional DICOM images. *Journal of Digital Imaging*, *17*, 205–216.

Sabaj, M. H. (Ed.). (2016). Standard symbolic codes for institutional resource collections in herpetology and ichthyology: An online reference. Version 6.5 (March 24, 2018). American Society of Ichthyologists and Herpetologists, Washington, D.C. Retrieved from http://www.asih.org.

Sire, J-Y. & Huysseune, A. (2003). Formation of dermal skeletal and dental tissues in fish: a comparative and evolutionary approach. *Biological Reviews*, *78*, 219–249.

Thiery, A. P., Shono, T., Kurokawa, D., Britz, R., Johanson, Z., & Fraser, G. (2017). Spatially restricted dental regeneration drives pufferfish beak development. *Proceedings of the National Academy of Sciences of the United States of America*, *114*(22), E4425–E4434. https://doi.org/10.1073/pnas.1702909114.

Trapani, J. (2001). Position of developing replacement teeth in teleosts. *Copeia*, *2001*(1), 35–51. https://doi.org/10.1643/0045-8511(2001)001[0035:PODRTI]2.0.CO;2

Tucker, D. W. (1956). Studies on the trichiuroid fishes – 3: A preliminary revision of the family Trichiuridae. *Bulletin of the British Museum of Natural History and Zoology*, *4*, 73.

How to cite this article: Bemis KE, Burke SM, St. John CA, Hilton EJ, Bemis WE. Tooth development and replacement in the Atlantic Cutlassfish, *Trichiurus lepturus*, with comparisons to other Scombroidei. *Journal of Morphology*. 2019;280:78–94. https://doi.org/10.1002/jmor.20919

APPENDIX: SPECIMENS EXAMINED

We studied specimens preserved in alcohol (A), decalcified-and-stained sections (DSS), dried osteological preparations (SD). All specimens examined are single specimen lots unless otherwise indicated. Total lengths (TL) are listed, if available. Institutional abbreviations follow Sabaj (2016).

Trichiuridae

Trichiurus lepturus: VIMS 35769 SD, 550 mm TL; VIMS 35770 SD, 514 mm TL; VIMS 35771 SD, 659 mm TL; VIMS 35772 SD, 614 mm TL; VIMS 35773 SD, 710 mm TL; VIMS 35774 SD, 650 mm TL; VIMS 35775 SD, 619 mm TL; VIMS 35776 SD, 540 mm TL; VIMS 35777 SD, 715 mm TL; VIMS 35778 SD, 695 mm TL; VIMS 35779 SD, 1103 mm TL; VIMS 35780 SD, 795 mm TL; VIMS 35781 SD, 670 mm TL; VIMS 35782 SD, 630 mm TL; VIMS 35783 SD, est. 570 mm TL; VIMS 35784 SD, 1034 mm TL; VIMS 35785 SD, 1068 mm TL; VIMS 35786 SD, 962 mm TL; VIMS 35787 SD, 1005 mm TL; VIMS 35788 SD, 1037 mm TL; VIMS 35789 SD, 964 mm TL; VIMS 35790 SD, 1000 mm TL; VIMS 35791 SD, 911 mm TL; VIMS 35792 SD, 1000 mm TL; VIMS 35793 SD, 1081 mm TL; VIMS 35794 SD, 1040 mm TL; VIMS 35795 SD, 948 mm TL; VIMS 35796 SD, est. 560 mm TL; VIMS 35797 SD, 806 mm TL; VIMS 35798 SD, 601 mm TL; VIMS 35799 SD, 590 mm TL; VIMS 35835 SD, 650 mm TL; VIMS 35836 SD, 668 mm TL; VIMS 35837 SD, 672 mm TL; VIMS 35838 SD, 670 mm TL; VIMS 35839 SD, 650 mm TL; VIMS 35840 SD, 598 mm TL; VIMS 35841 SD, 650 mm TL; VIMS 35842 SD, 653 mm TL; VIMS 35843 SD, 580 mm TL; VIMS 35844 SD, 575 mm TL; VIMS 35845 SD, 593 mm TL; VIMS 35846 SD, 640 mm TL; VIMS 35847 SD, 620 mm TL; VIMS 35848 SD, 745 mm TL; VIMS 35849 SD, 556 mm TL; VIMS 35850 SD, 620 mm TL; VIMS 35851 SD, 570 mm TL; VIMS 35852 SD, 640 mm TL; VIMS 35853 SD, 566 mm TL; VIMS 35854 SD, 630 mm TL; VIMS 35855 SD, 560 mm TL; VIMS 35856 SD, 630 mm TL; VIMS 35857 SD, 608 mm TL; VIMS 35858 SD, 553 mm TL; VIMS 35859 SD, 640 mm TL; VIMS 35860 SD, 584 mm TL; VIMS 35861 SD, 675 mm TL; VIMS 35862 SD, 1050 mm TL; VIMS 35863 SD, 830 mm TL; VIMS 35864 SD, 873 mm TL; VIMS 35865 SD, 759 mm TL; VIMS 35866 SD, 1041 mm TL; VIMS 35867 SD, 946 mm TL; VIMS 35868 SD, 940 mm TL; VIMS 35869 SD, 1045 mm TL; VIMS 35870 SD, 1068 mm TL; VIMS 35871 SD, est. 985 mm TL; VIMS 35872 SD, 906 mm TL; VIMS 35873 SD, 916 mm TL; VIMS 35874 SD, 535 mm TL, VIMS 35894 A, *n* = 3, 600 mm TL, 641 mm TL, 718 mm TL; VIMS 35901 A, *n* = 2, TL unknown; VIMS 35823 A, *n* = 2, 240 mm TL, 220 mm SL.

SML 450916-000 A, *n* = 4, 5.7 mm TL, 5.8 mm TL, 5.9 mm TL, 5.9 mm TL; SML 39772-000 A, 39 mm TL; SML 18590-000 A, 22.6 mm TL, SML 300582-000 A, *n* = 2, 22.13 mm TL, 28.90 mm TL; SML 18583-000 A, 10.6 mm TL, SML 450839-000 42537 A, 49.6 mm TL.

Lepidopus caudatus: AMNH I-91527 SD; AMNH I-98413 SD.

Gempylidae

Lepidocybium flavobrunneum: AMNH I-214575 SD; AMNH I-93584 SD.

Neoepinnula americana: VIMS 35898 A (2) 184 mm TL, 206 mm TL; VIMS 35900 A (3) 178 mm TL, 184 mm TL, 182 mm TL; VIMS 35903 A (2) 155 mm TL, 121 mm TL.

Nesiarchus nasutus: VIMS 35895, A 315 mm TL.

Gempylus serpens: AMNH I-90897 SD; AMNH I-90898 SD; AMNH I-216465 SD.

Promethichthys prometheus: AMNH I-210600 SD; VIMS 35896 A 345 mm TL; VIMS 35897 A 203 mm TL; VIMS 35899 A, *n* = 2, 225 mm TL, 211 mm TL.

Rexea solandri: AMNH I-91984 SD; AMNH I-214360 SD.

Scombridae

Acanthocybium solanderi: AMNH I-79804 SD; AMNH I-57641 SD.

Auxis rochi: AMNH I-88912 SD; AMNH I-56704 SD.

Auxis thazard: AMNH I-56712SD.

Euthynnus affinis: AMNH I-217951 SD; AMNH I-217948 SD.

Gasterochisma melampus: AMNH I-98426 SD; AMNH I-93480 SD; AMNH I-093411 SD.

Grammatorcynus bicarinatus: AMNH I-214132 SD.

Katsuwonus pelamis: AMNH I-219988 SD.

Scomberomorus maculatus: CUMV 79384 SD.

Scomberomorus cavalla: AMNH I-79721 SD.

Scomber scombrus: AMNH I-55859 SD, *n* = 5.

Thunnus atlanticus: AMNH I-79718 SD; AMNH I-79802 SD; AMNH I-79801 SD.

Scombrolabracidae

Scombrolabrax heterolepis: AMNH I-79557 SD; AMNH I-218211 SD; AMNH I-211557 SD.

Pomatomidae

Pomatomus saltatrix: CUMV 97588 SD; CUMV 97589 SD; CUMV 97590 SD; CUMV 97591 SD.